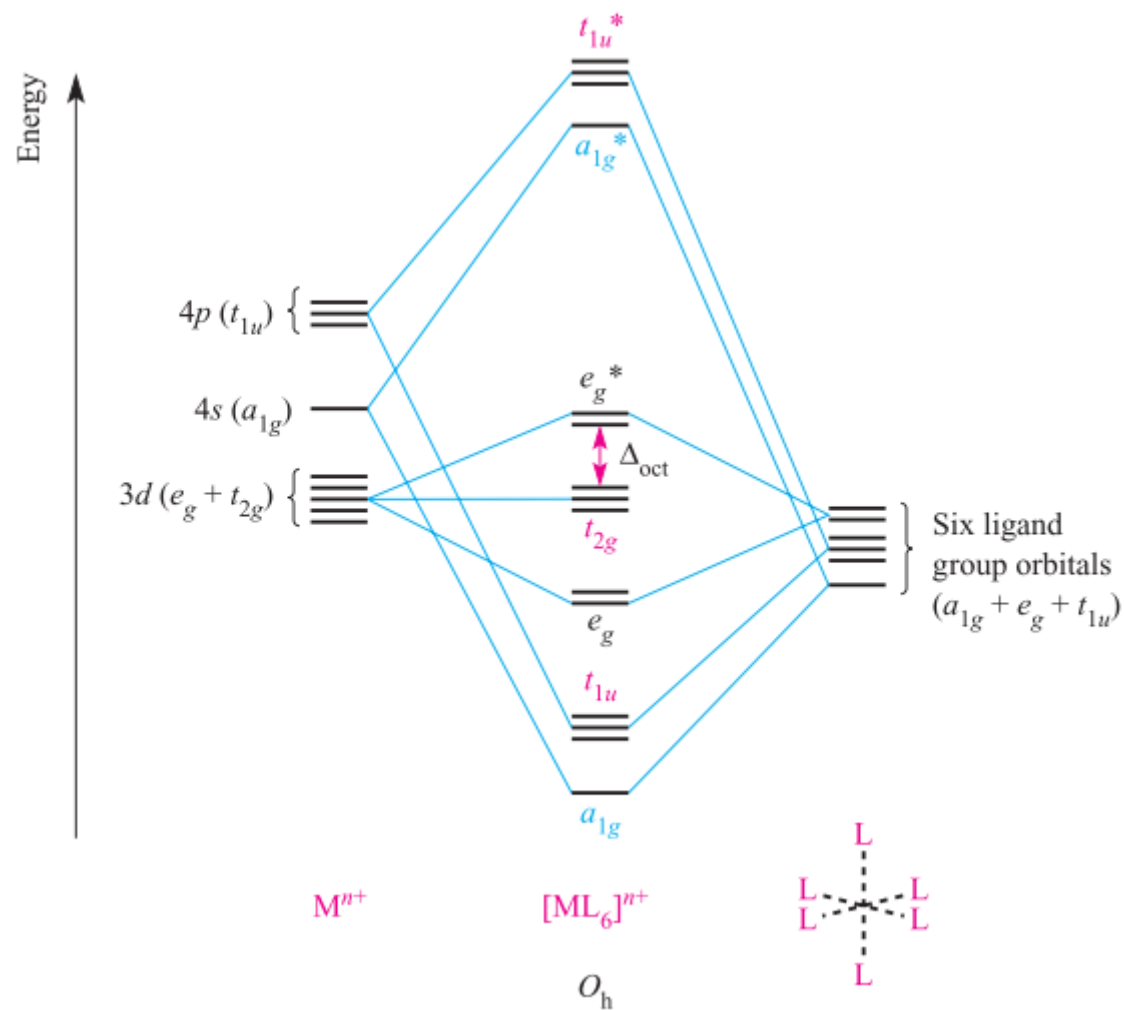
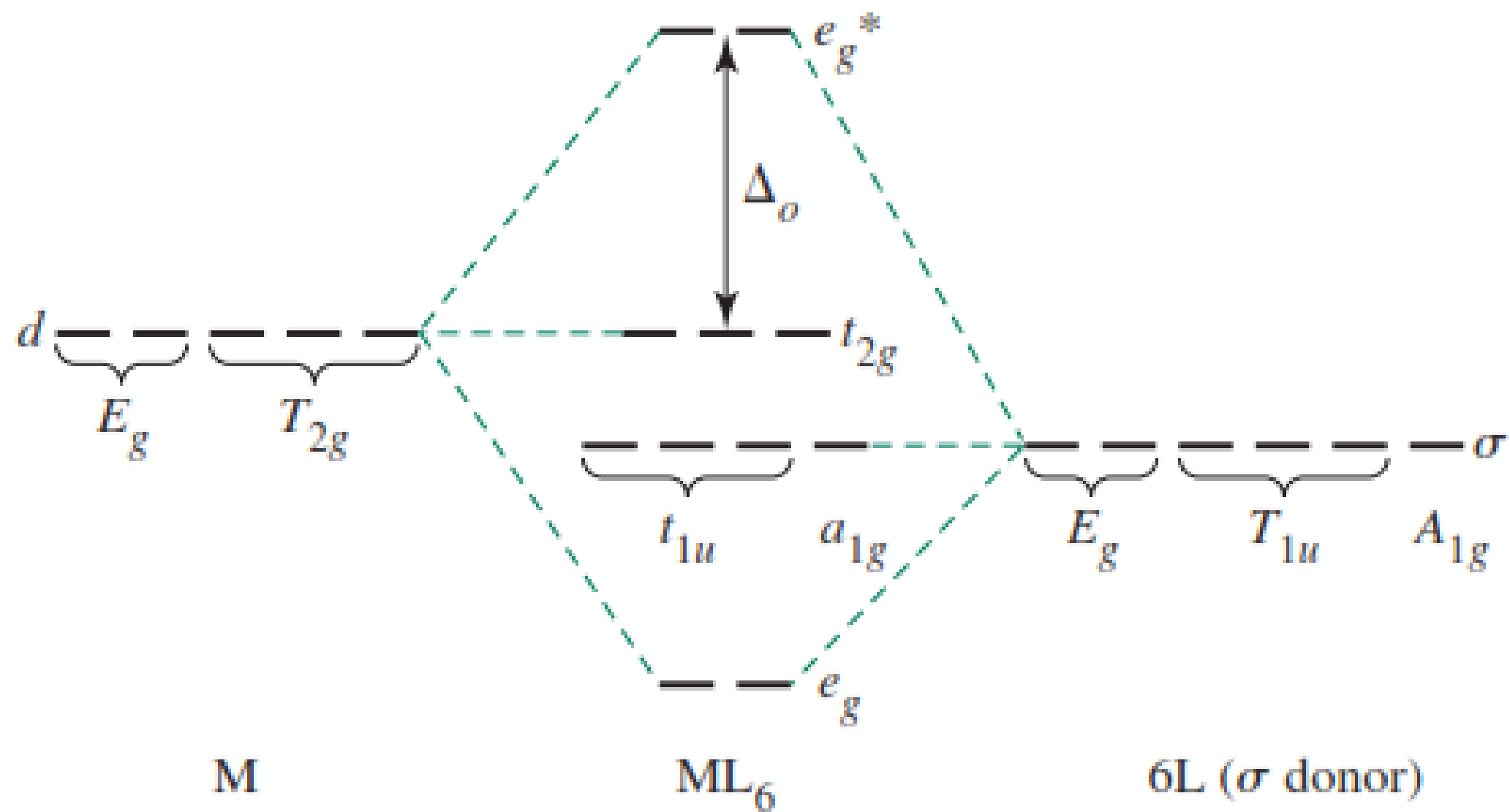


Molecular orbital theory

Complexes with *no* metal–ligand π -bonding



Metal orbital	Symmetry label	Degeneracy
s	a_{1g}	1
p_x, p_y, p_z	t_{1u}	3
$d_{x^2-y^2}, d_{z^2}$	e_g	2
d_{xy}, d_{yz}, d_{zx}	t_{2g}	3



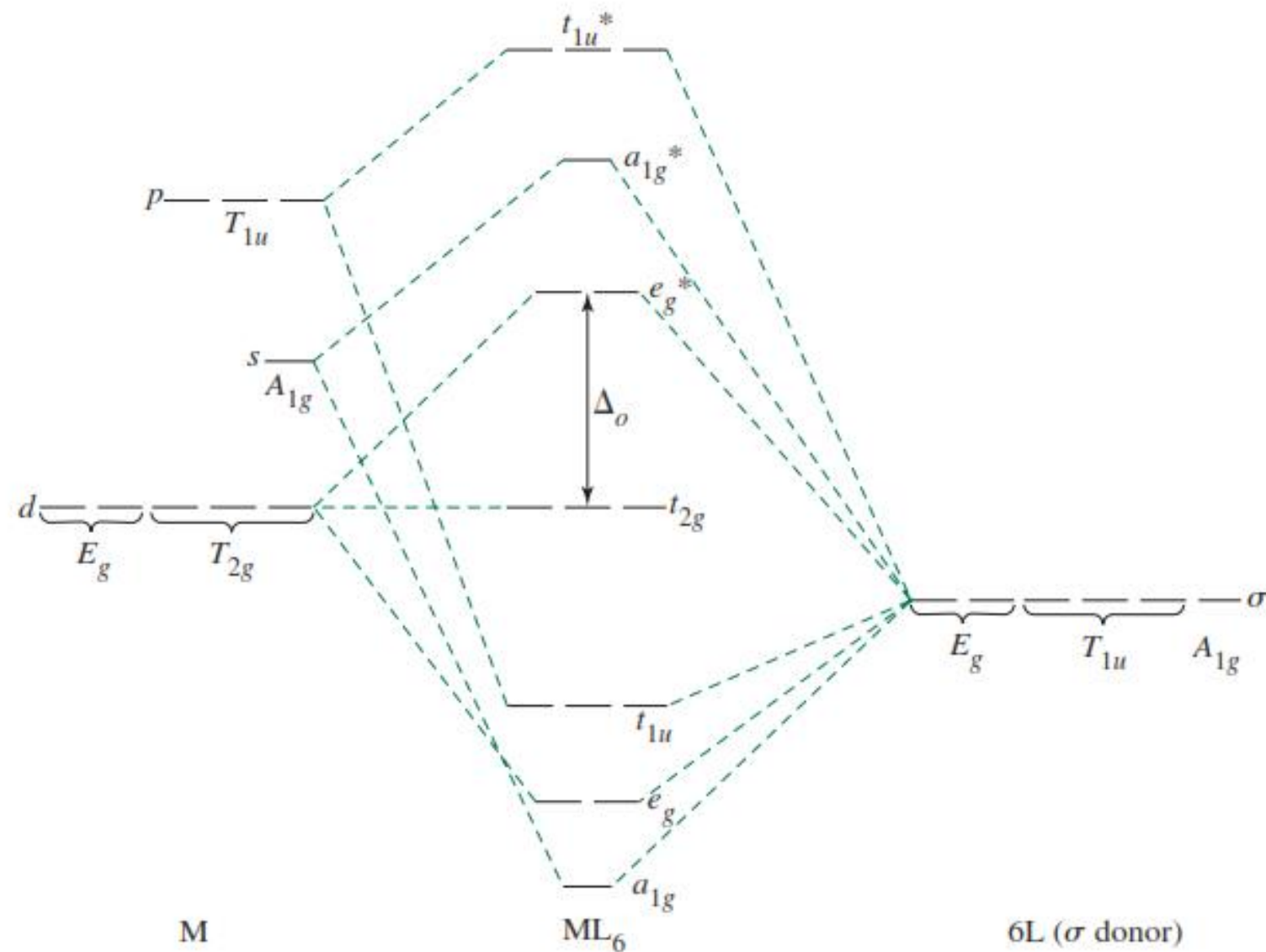


FIGURE 10.5 Sigma-Donor Interactions with Metal s , p , and d Orbitals. As in Chapter 5, the symmetry labels of the atomic orbitals are capitalized, and the labels of the molecular orbitals are in lowercase. The six filled ligand donor orbitals contribute 12 electrons to the lowest six molecular orbitals in this diagram. The metal valence electrons occupy the t_{2g} and, possibly, e_g^* orbitals.

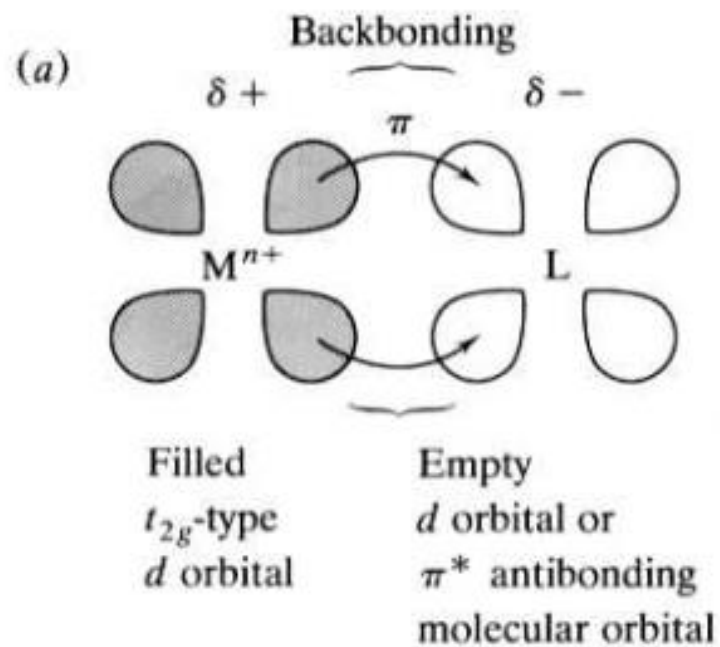
Complexes with metal–ligand π -bonding

A π -donor ligand donates electrons to the metal centre in an interaction that involves a filled ligand orbital and an empty metal orbital; a π -acceptor ligand accepts electrons from the metal centre in an interaction that involves a filled metal orbital and an empty ligand orbital.

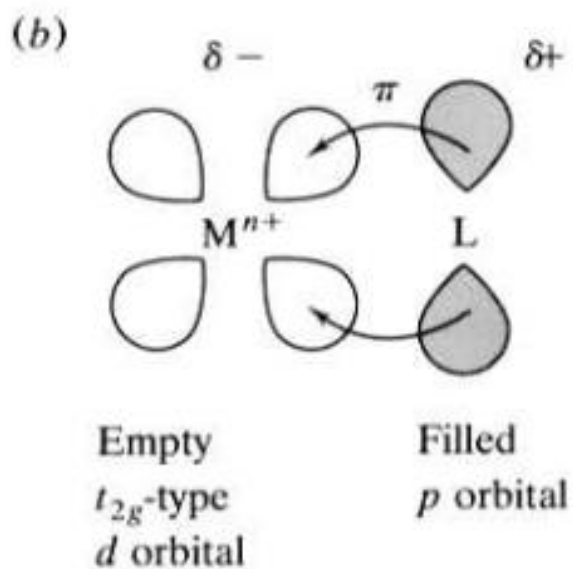
π -Donor ligands include Cl^- , Br^- and I^-

π -acceptor ligands are CO , N_2 , NO

π donor	weak π donor	no π effects	π acceptor
I^- , Br^- , Cl^- , F^-	H_2O	NH_3	PR_3 , CO

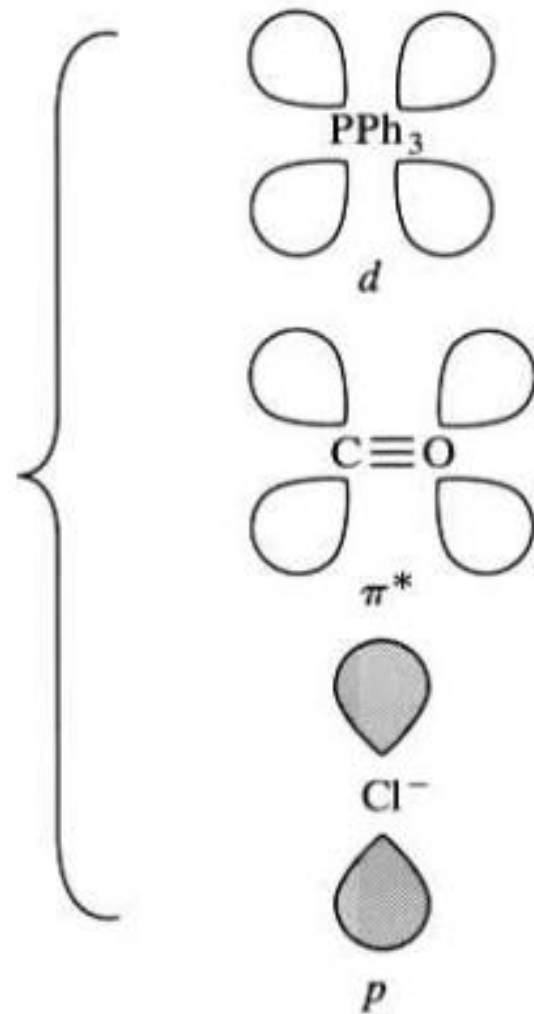
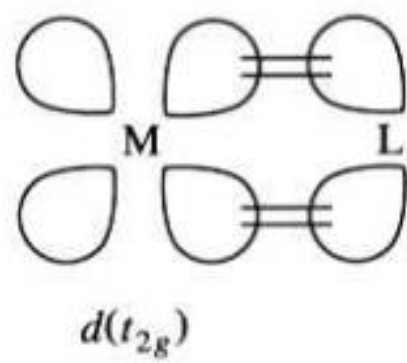


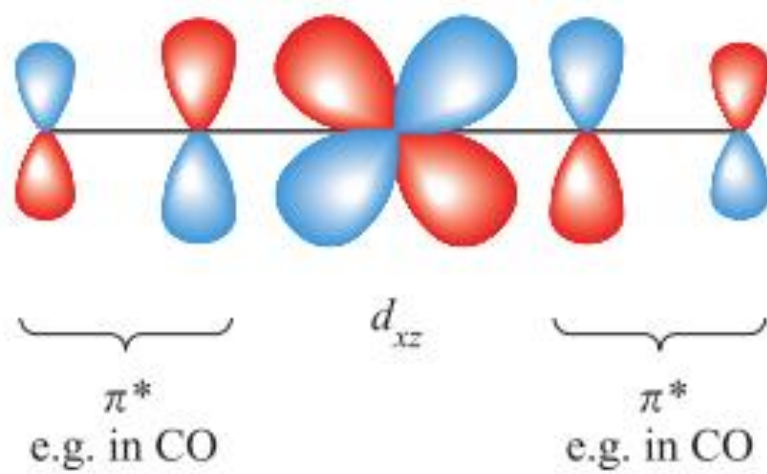
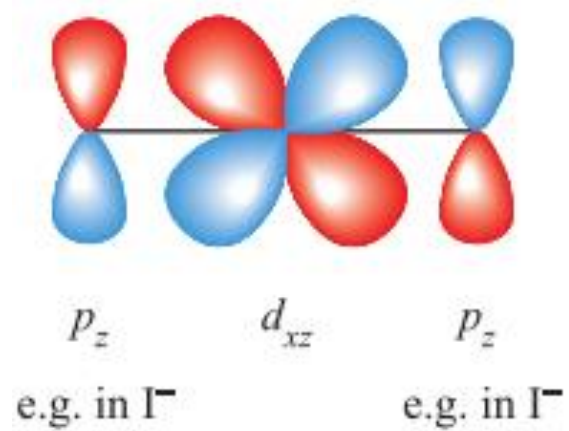
$M \rightarrow L$ electron flow increases the polarity of the $M-L$ bond and makes L more capable of splitting metal d orbitals

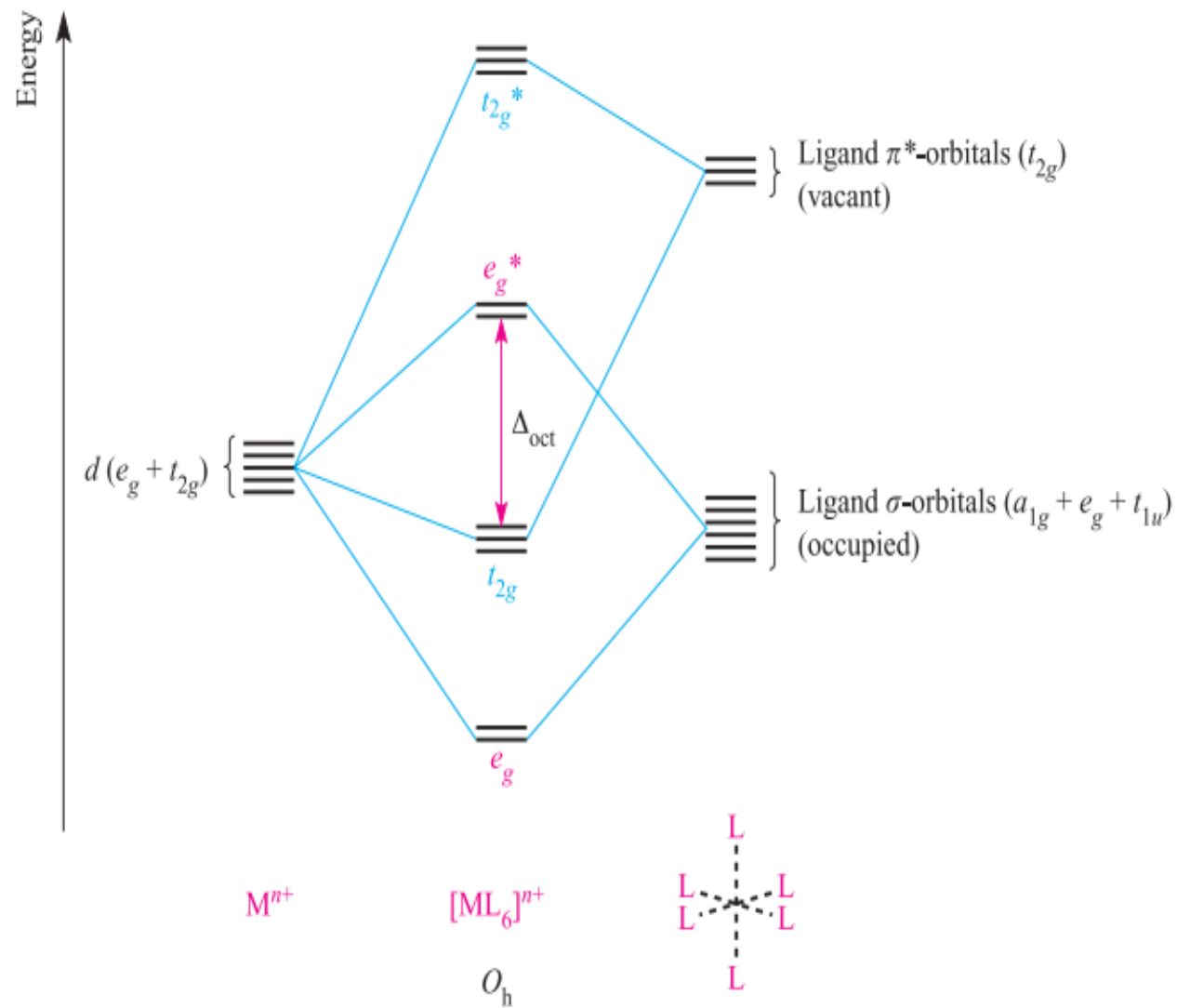
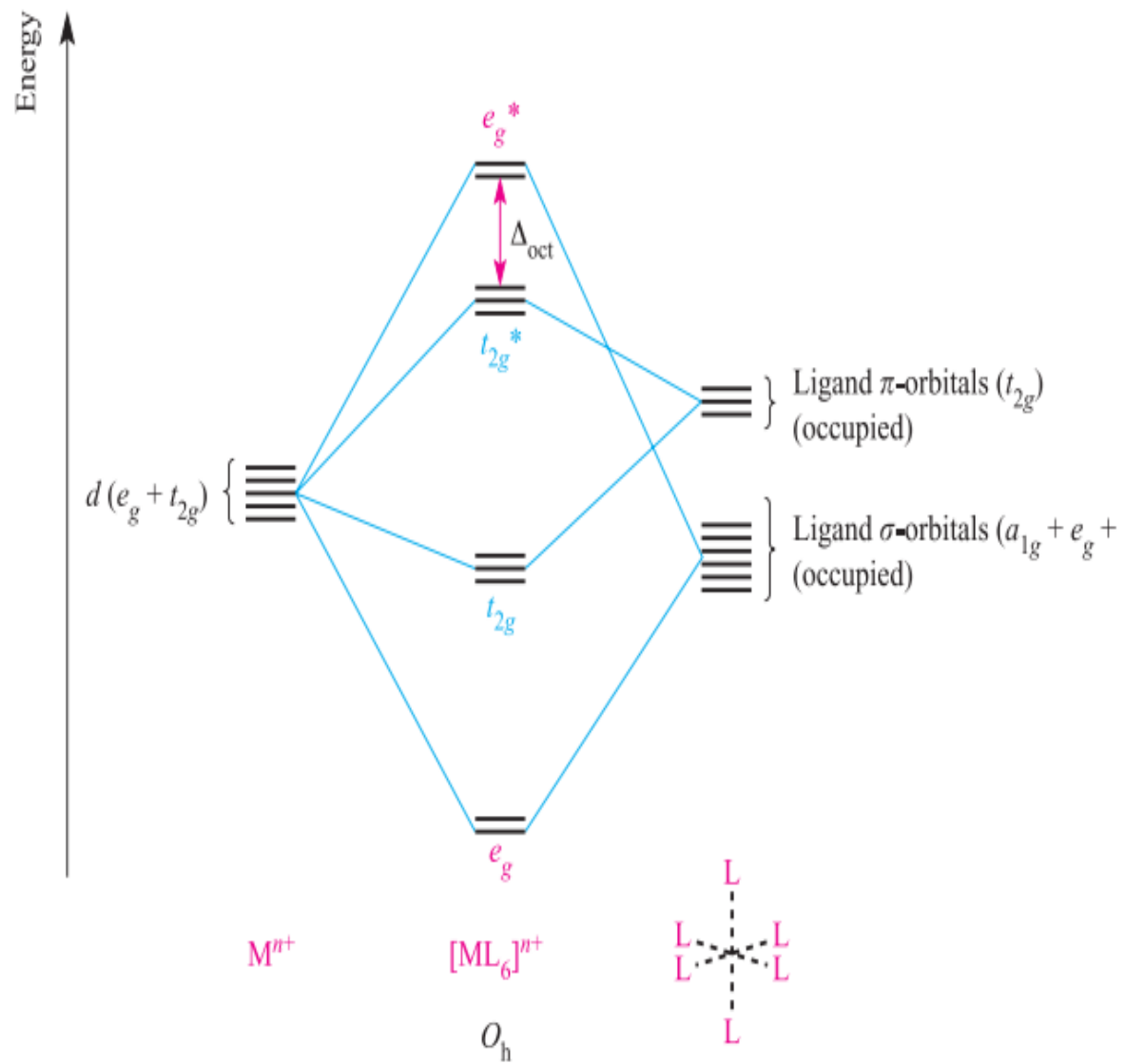


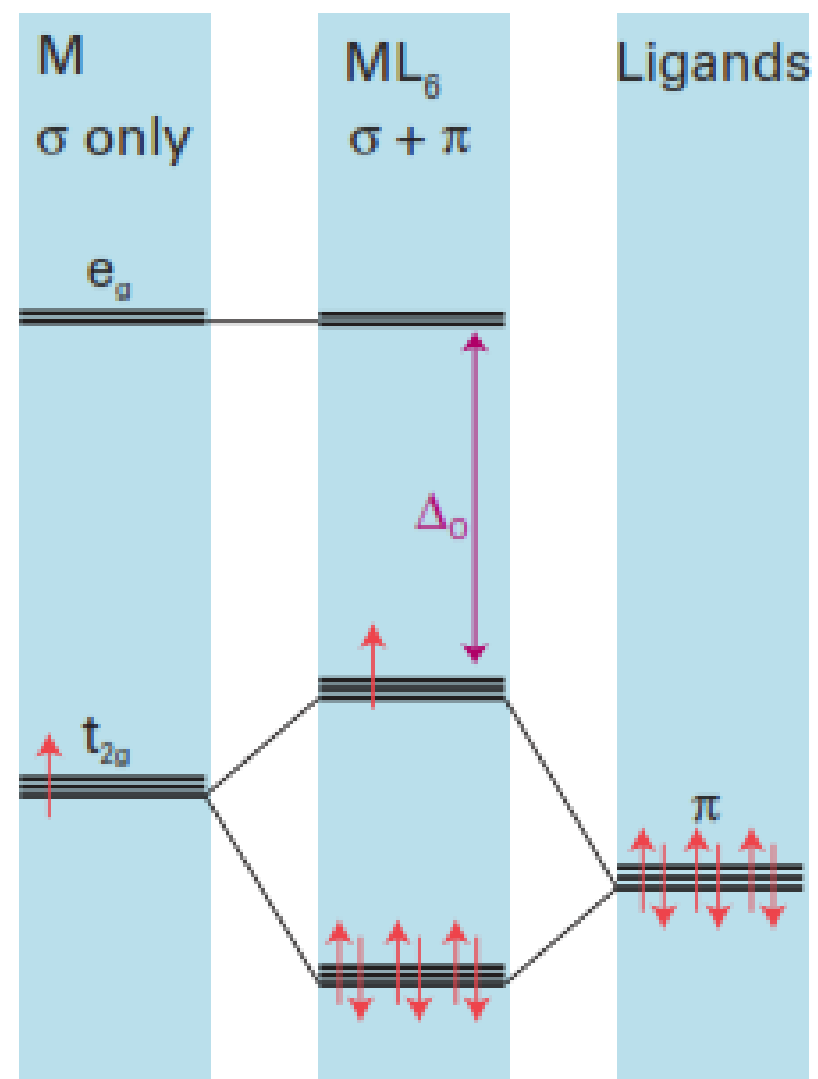
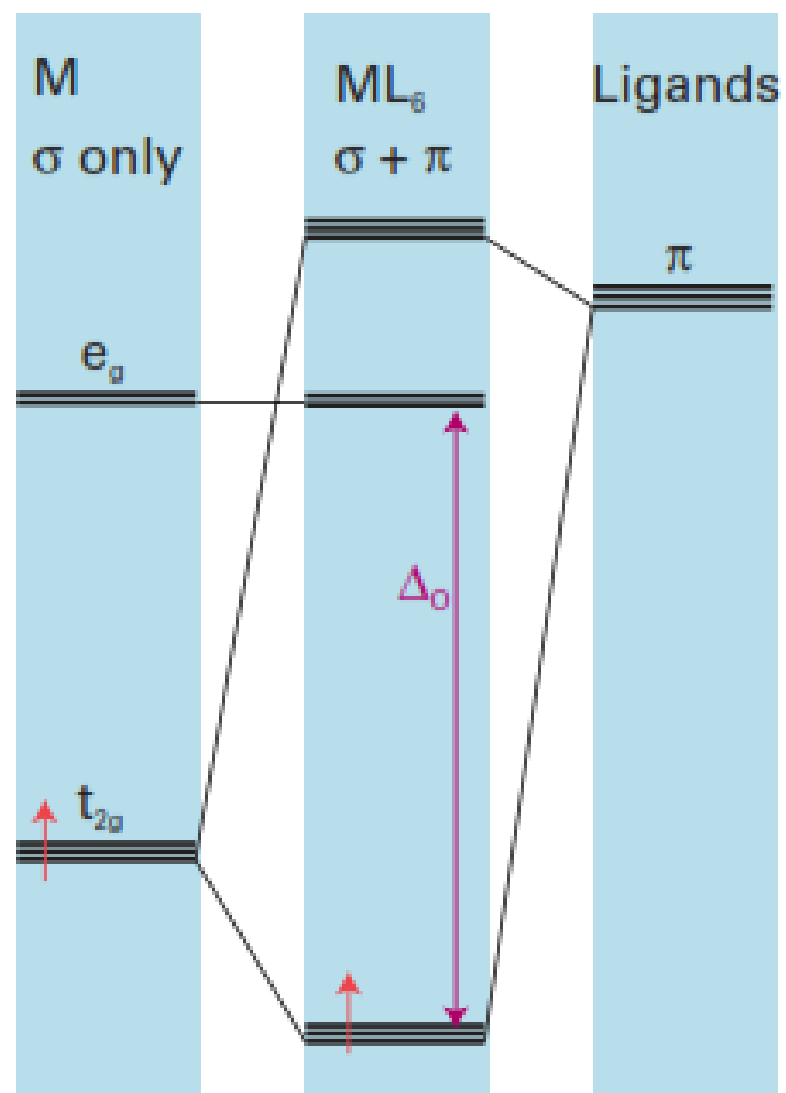
$M \leftarrow L$ electron flow decreases the polarity of the $M-L$ bond and makes L less capable of splitting metal d orbitals

π -type covalent interactions:









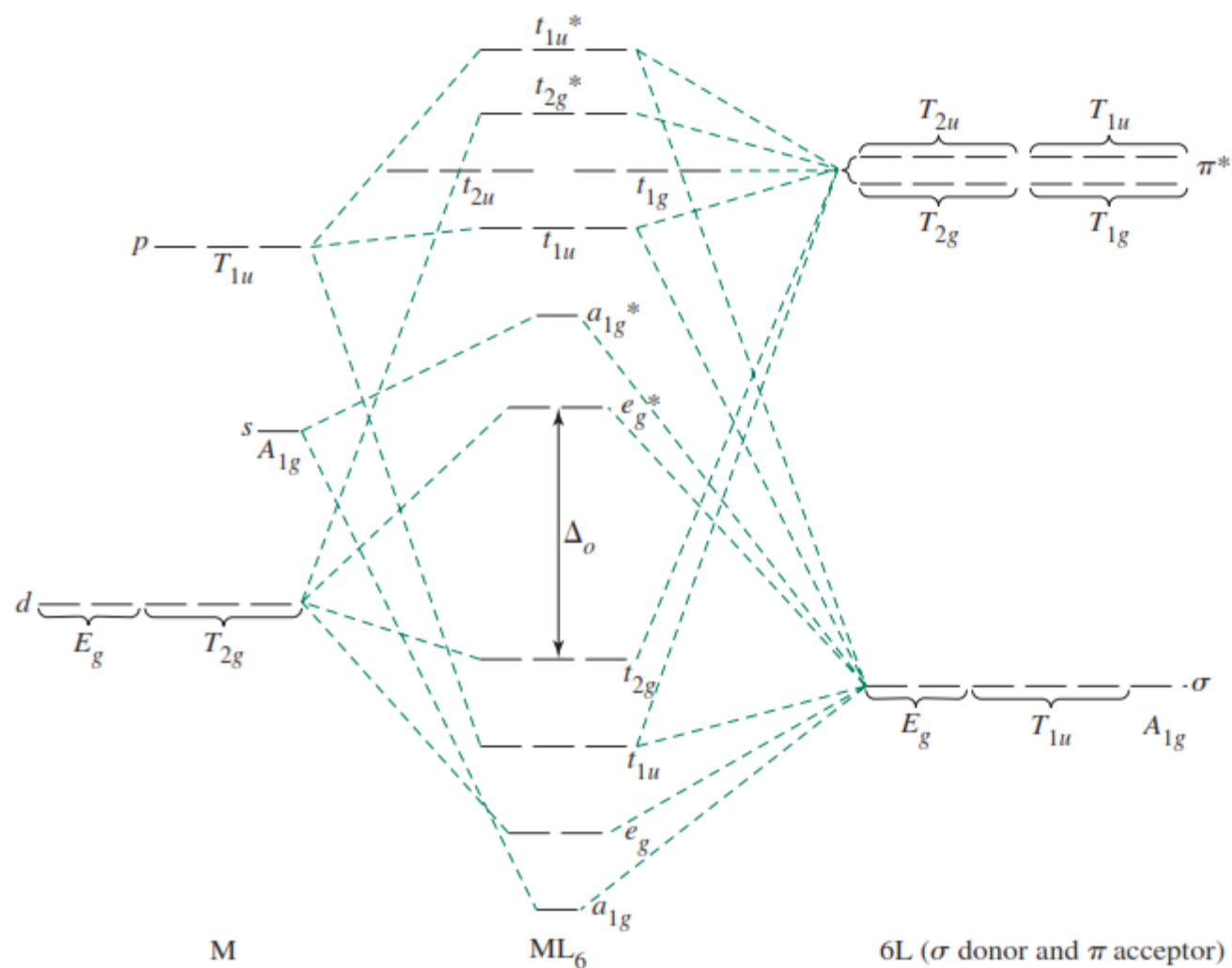
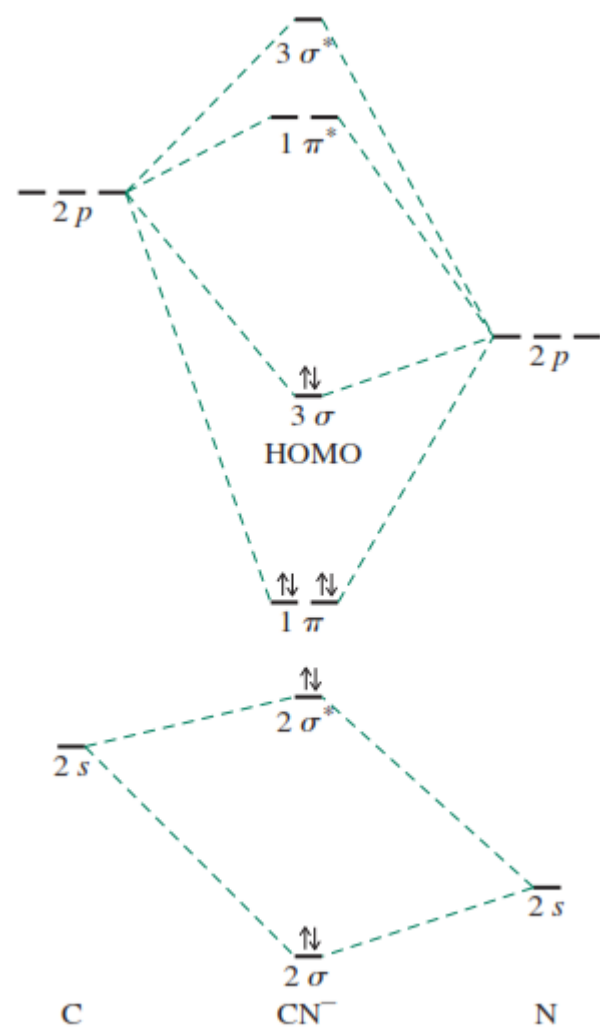
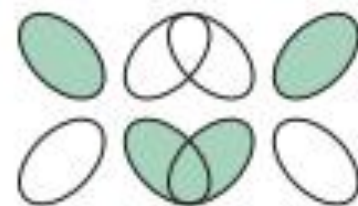


FIGURE 10.7 Sigma-Donor and π -Acceptor Interactions in an Octahedral Complex.* The six filled ligand donor orbitals contribute 12 electrons to the lowest six molecular orbitals in this diagram. The metal valence electrons occupy the t_{2g} , now π -bonding orbitals, and possibly the e_g^* orbitals.



Representative
metal orbital

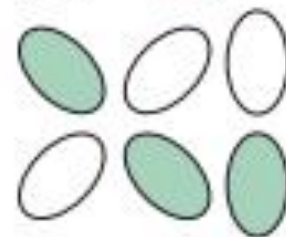
d_{yz}



d_{yz}

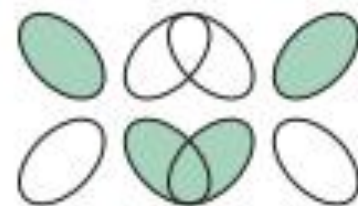


d_{yz}



Representative
ligand orbital

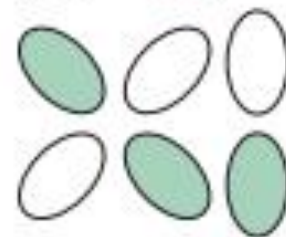
d_{yz}

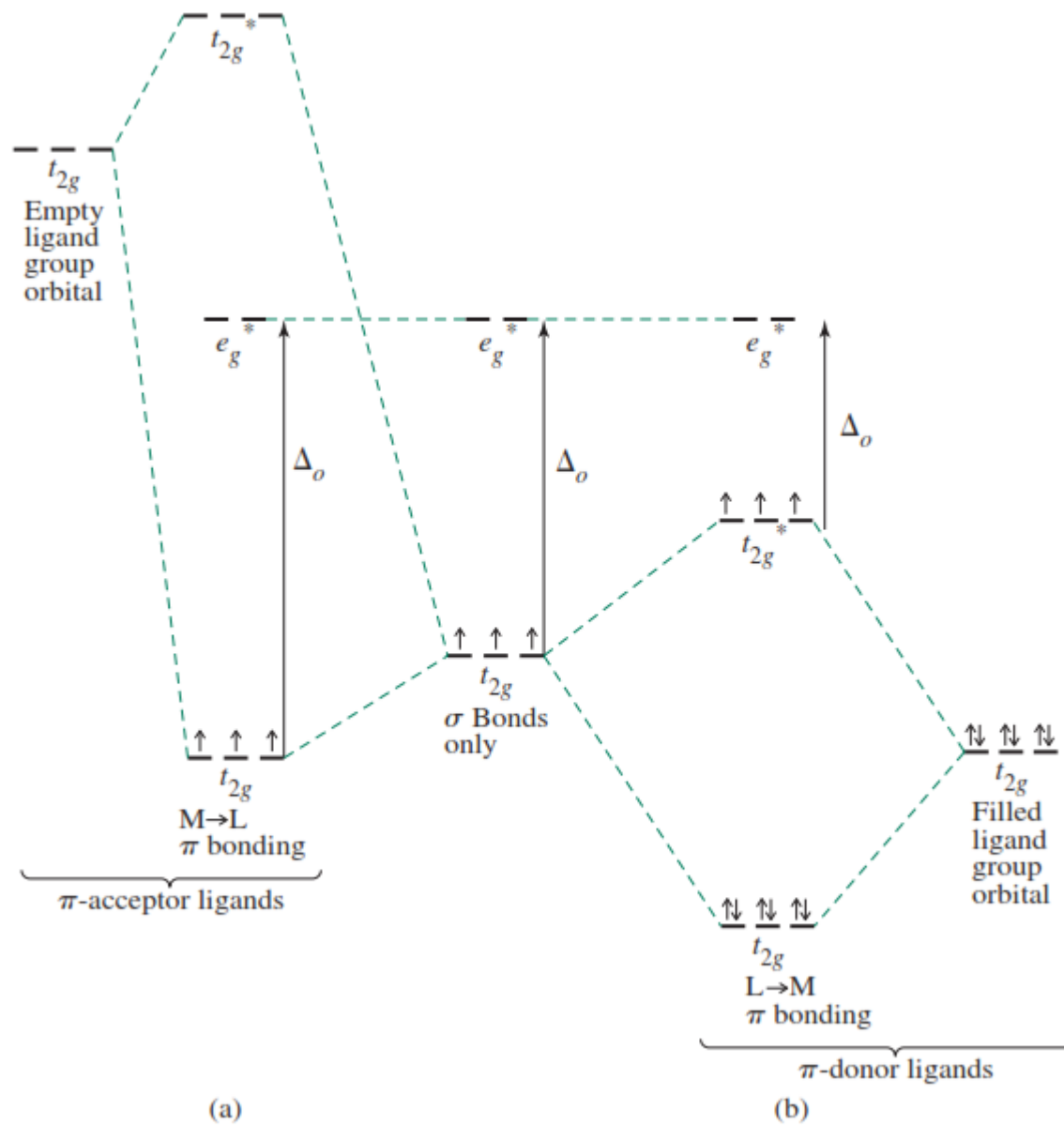


π_z^*



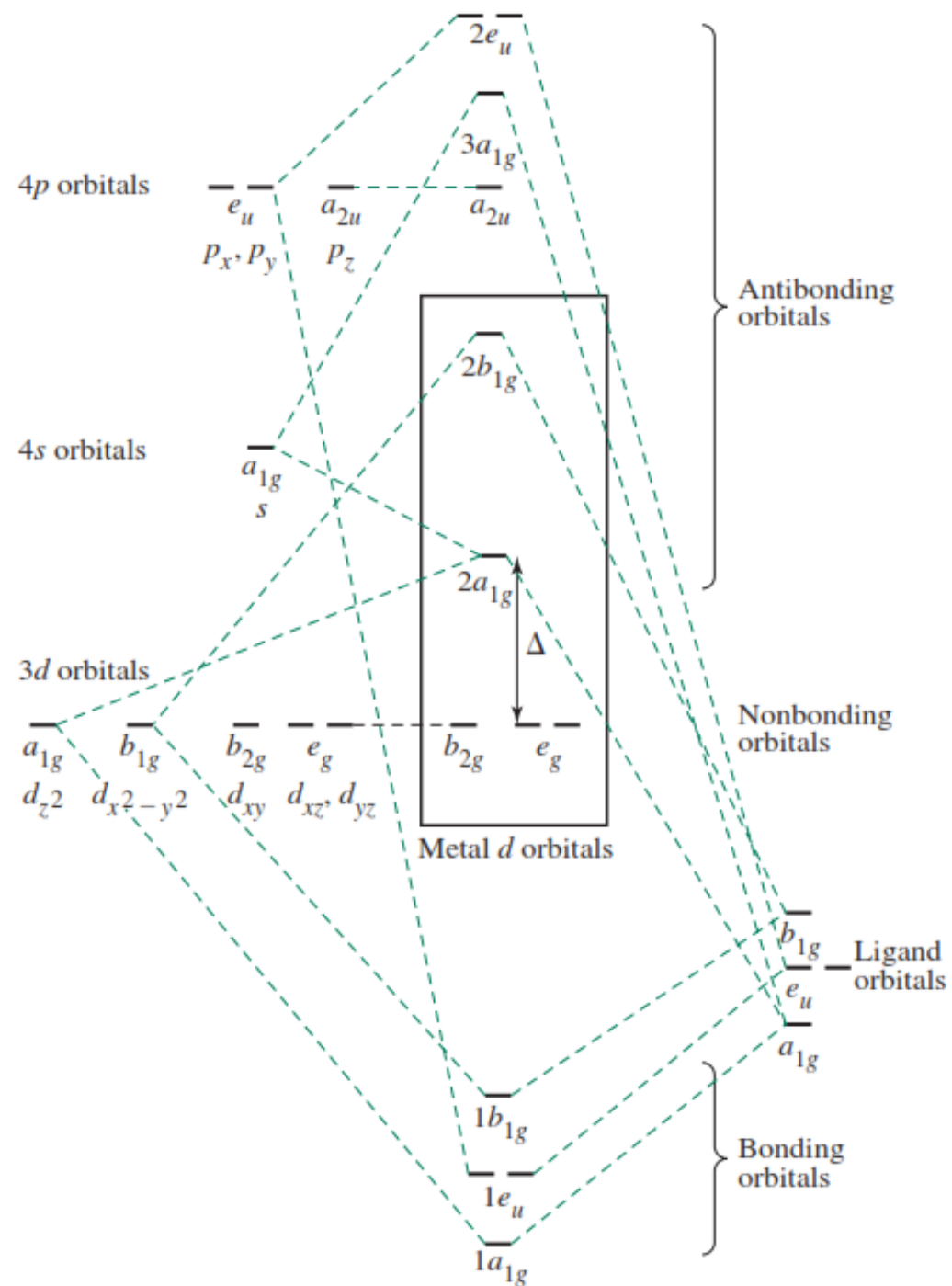
p_z

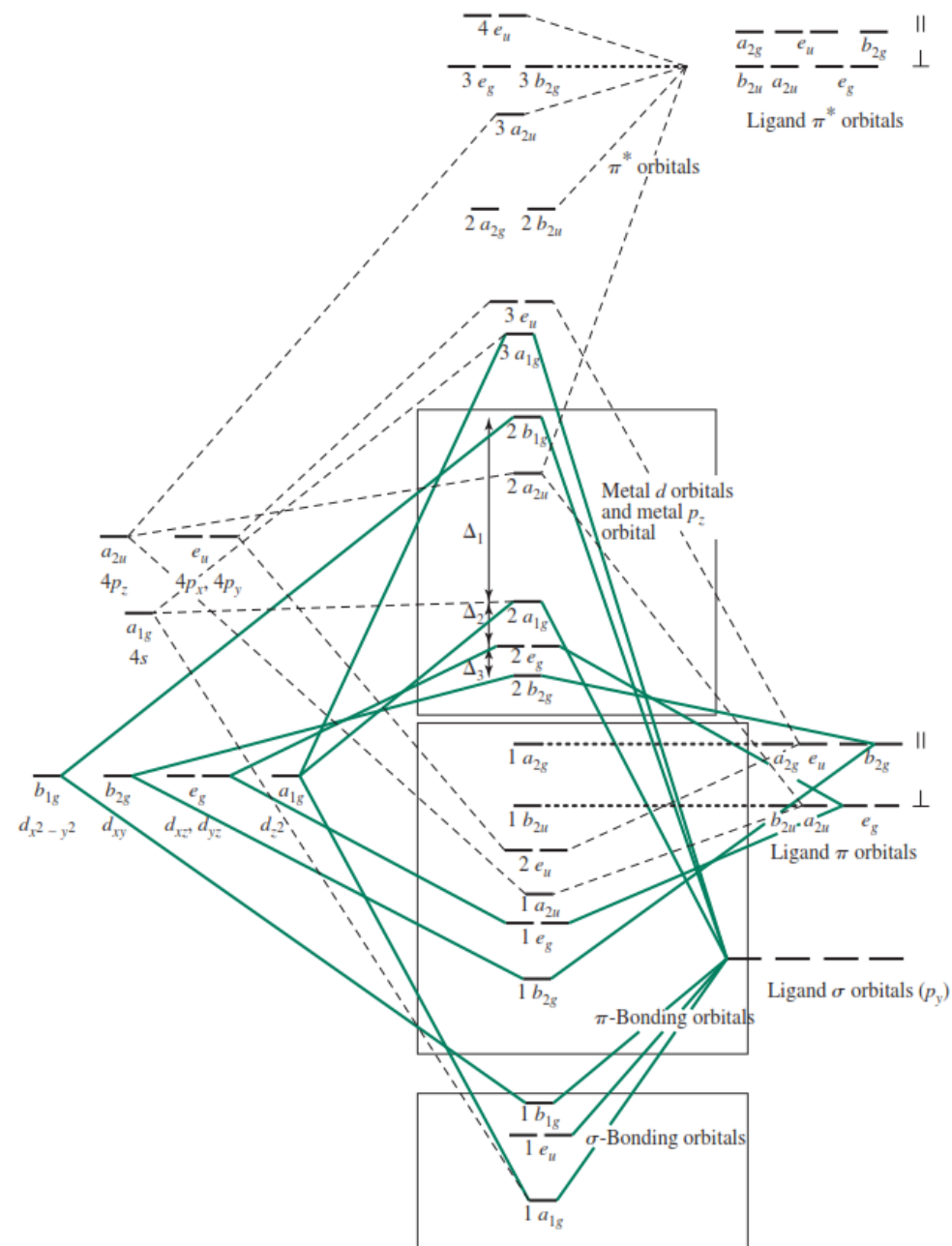




- Δ_{oct} *decreases* in going from a σ -complex to one containing π -donor ligands;
- for a complex with π -donor ligands, increased π -donation stabilizes the t_{2g} level and destabilizes the t_{2g}^* , thus decreasing Δ_{oct} ;
- Δ_{oct} values are relatively large for complexes containing π -acceptor ligands, and such complexes are likely to be low-spin;
- for a complex with π -acceptor ligands, increased π -acceptance stabilizes the t_{2g} level, increasing Δ_{oct} .

Square-Planar Complexes

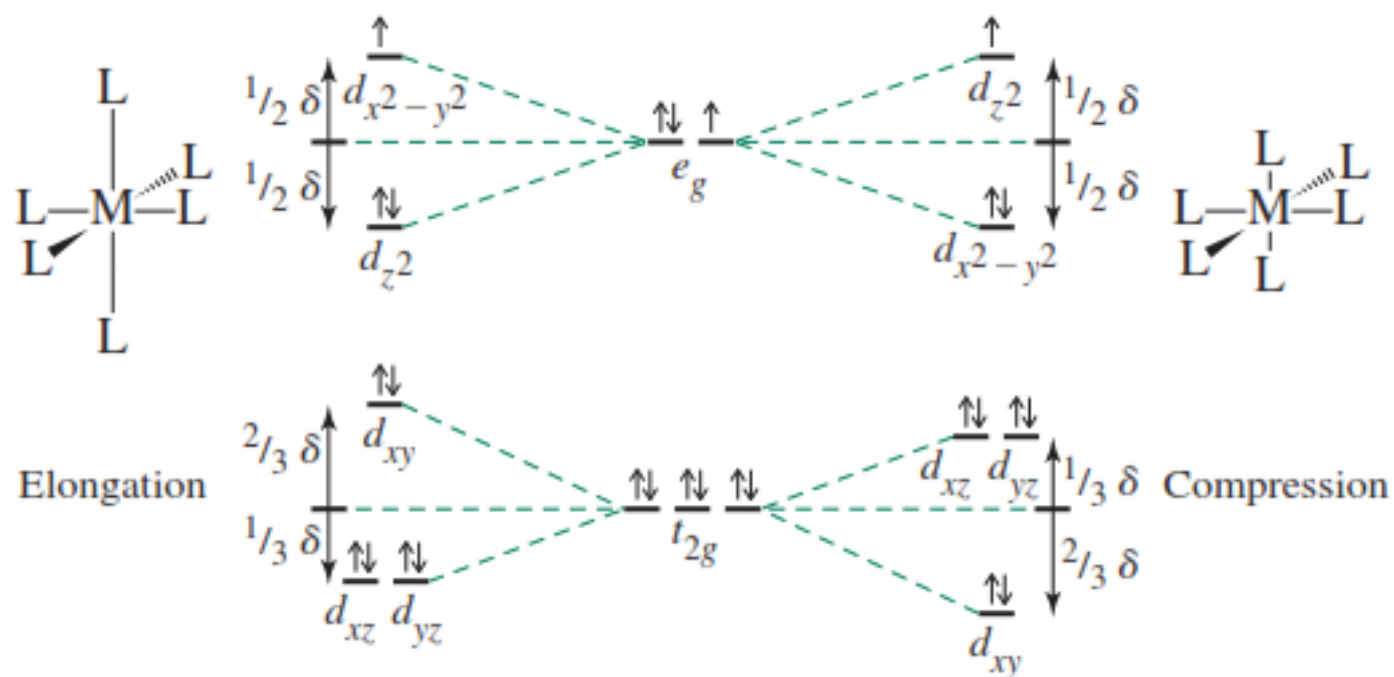




The Jahn–Teller Effect

Number of Electrons	1	2	3	4	5	6	7	8	9	10
High-spin Jahn–Teller	w	w		s		w	w		s	
Low-spin Jahn–Teller	w	w		w	w		s		s	

w = weak Jahn–Teller effect expected (t_{2g} orbitals unevenly occupied); s = strong Jahn–Teller effect expected (e_g orbitals unevenly occupied); No entry = no Jahn–Teller effect expected.

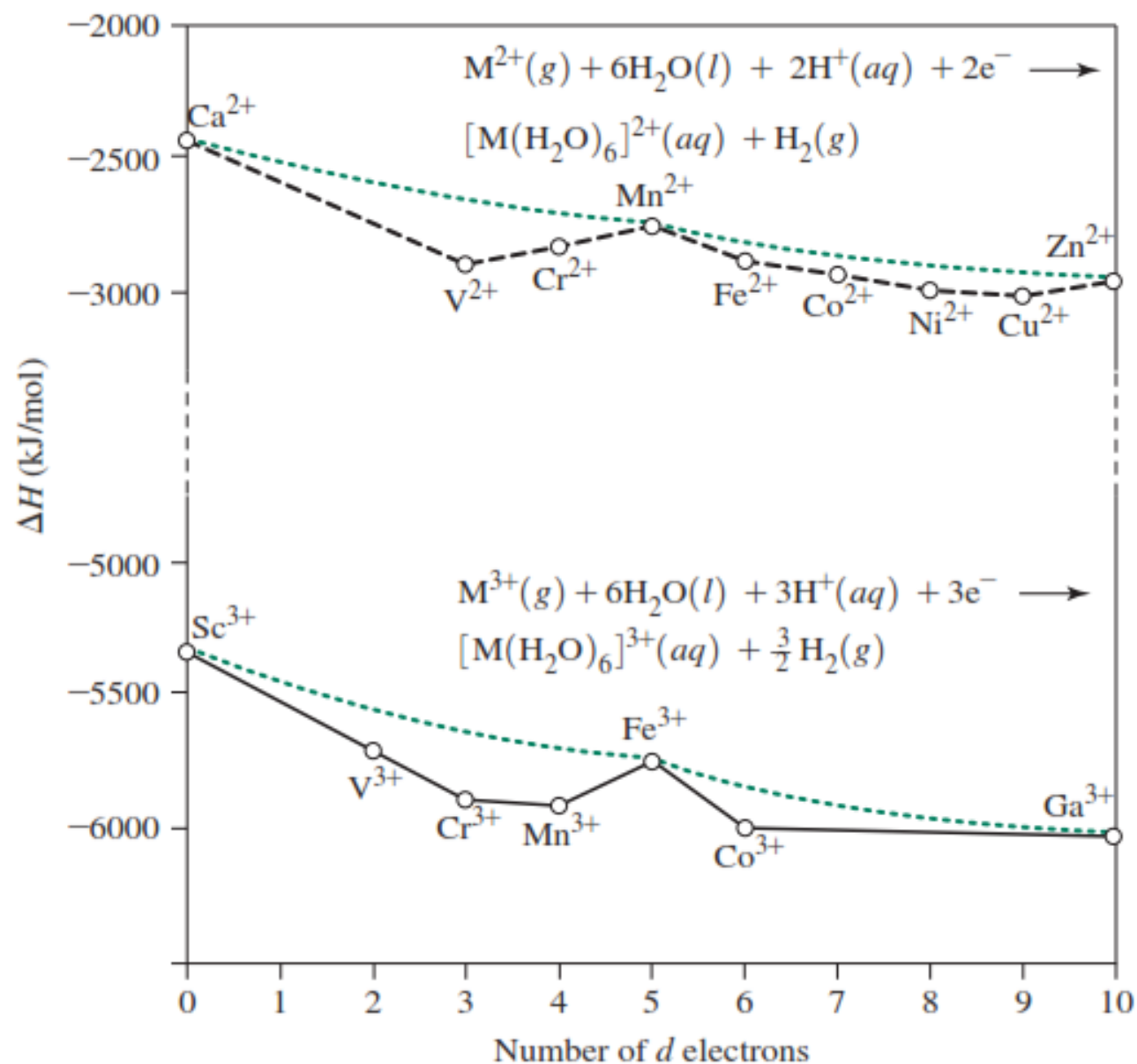


Evidence for Electronic Structures

TABLE 10.2 Thermodynamic Data for Monodentate vs. Bidentate Ligand Substitution Reactions at 25 °C

Reactants	Product	ΔH° (kJ/mol)	ΔS° (J/mol K)	ΔG° (kJ/mol) $\Delta H^\circ - T\Delta S^\circ$	K
$[\text{Cd}(\text{H}_2\text{O})_6]^{2+}$					
4 CH_3NH_2	$[\text{Cd}(\text{CH}_3\text{NH}_2)_4(\text{H}_2\text{O})_2]^{2+}$	-57.3	-67.3	-37.2	3.3×10^6
2 en	$[\text{Cd}(\text{en})_2(\text{H}_2\text{O})_2]^{2+}$	-56.5	+14.1	-60.7	4.0×10^{10}
$[\text{Cu}(\text{H}_2\text{O})_6]^{2+}$					
2 NH_3	$[\text{Cu}(\text{NH}_3)_2(\text{H}_2\text{O})_4]^{2+}$	-46.4	-8	-43.9	4.5×10^7
en	$[\text{Cu}(\text{en})(\text{H}_2\text{O})_4]^{2+}$	-54.4	+23	-61.1	4.4×10^{10}

FIGURE 10.12 Enthalpies of Hydration of Transition-Metal Ions. The lower curves show experimental values for individual ions; the blue upper curves result when the LFSE, as well as contributions from spin-orbit splitting, a relaxation effect from contraction of the metal–ligand distance, and interelectronic repulsion energy are subtracted. (Data from D. A. Johnson and P. G. Nelson, *Inorg. Chem.*, **1995**, 34, 5666 (M^{2+} data); and D. A. Johnson and P. G. Nelson, *Inorg. Chem.*, **1999**, 4949 (M^{3+} data).)



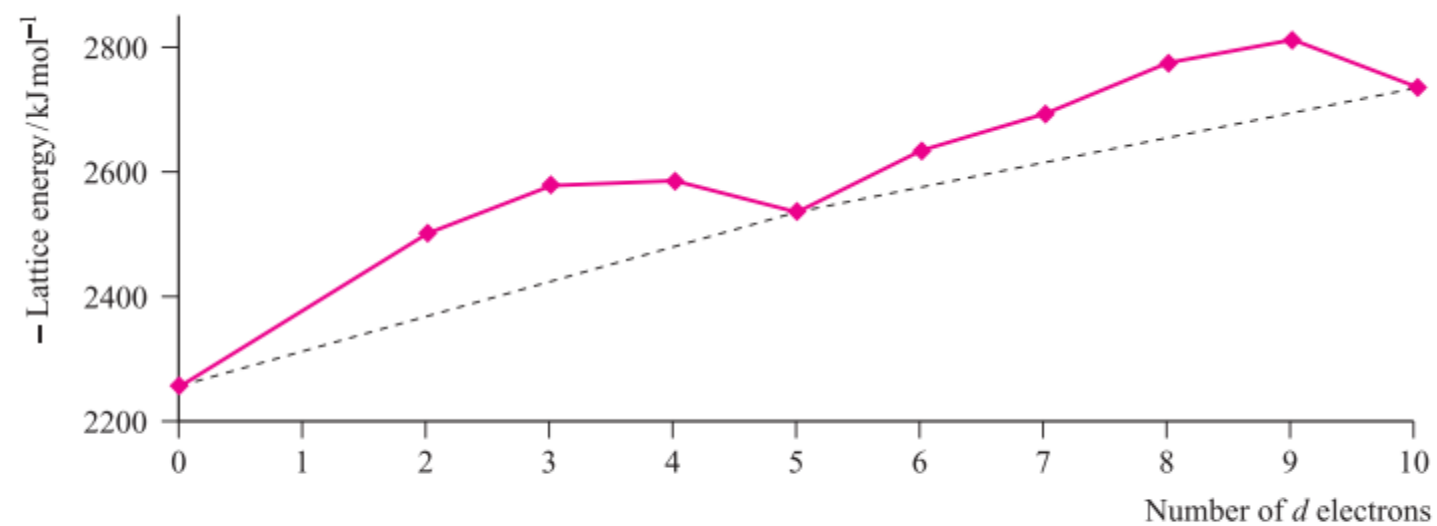


Fig. 20.27 Lattice energies (derived from Born–Haber cycle data) for MCl_2 where M is a first row *d*-block metal; the point for d^0 corresponds to CaCl_2 . Data are not available for scandium where the stable oxidation state is +3.

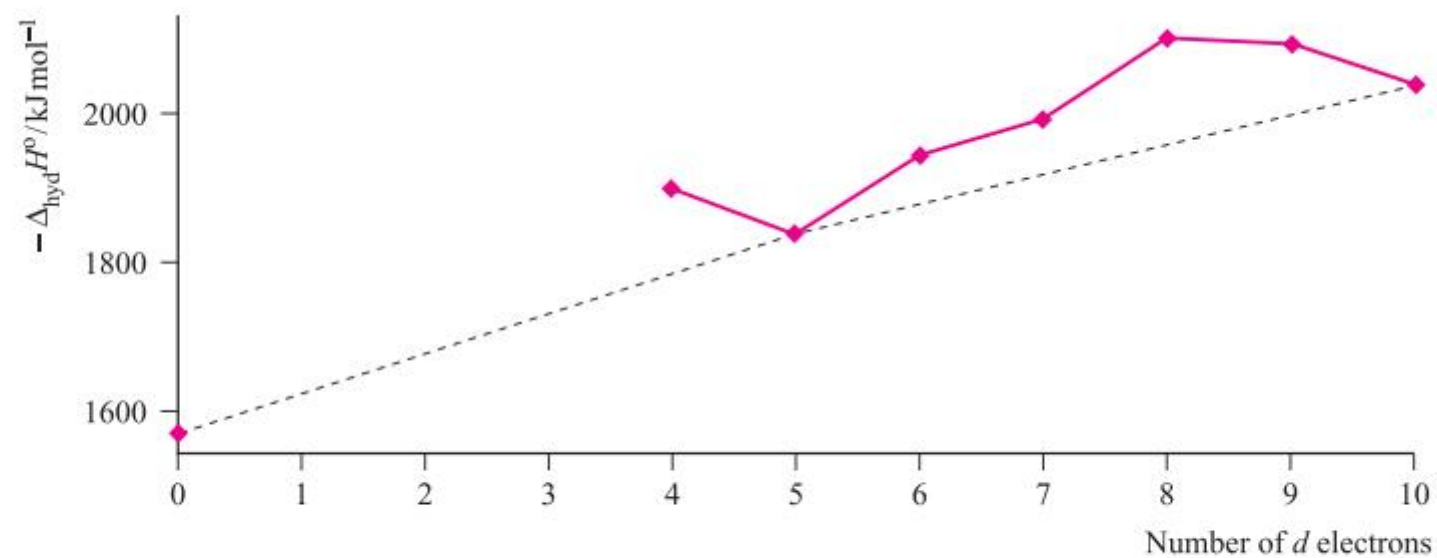
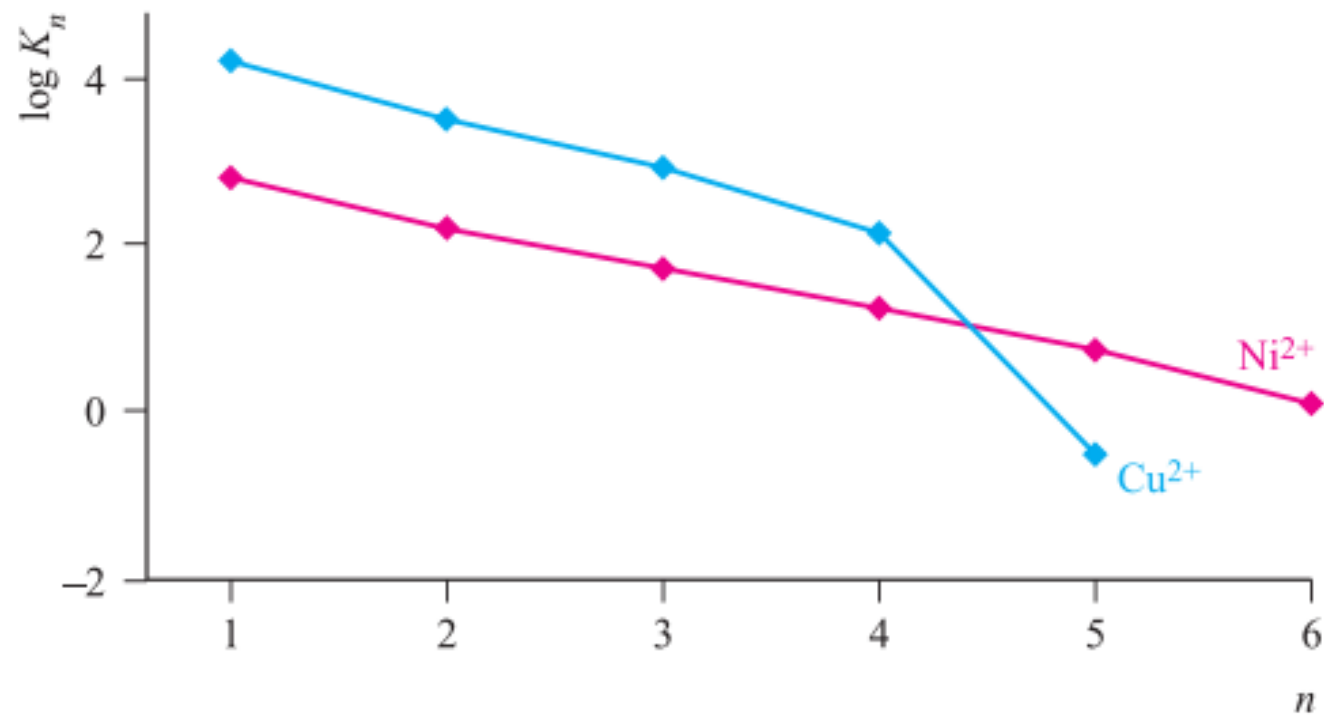
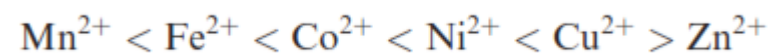


Fig. 20.28 Absolute enthalpies of hydration of the M^{2+} ions of the first row metals; the point for d^0 corresponds to Ca^{2+} . Data are not available for Sc^{2+} , Ti^{2+} and V^{2+} .

Table 20.10 Overall stability constants for selected high-spin *d*-block metal complexes.

Metal ion	Mn ²⁺	Fe ²⁺	Co ²⁺	Ni ²⁺	Cu ²⁺	Zn ²⁺
log β_3 for [M(en) ₃] ²⁺	5.7	9.5	13.8	18.6	18.7	12.1
log β for [M(EDTA)] ²⁻	13.8	14.3	16.3	18.6	18.7	16.1



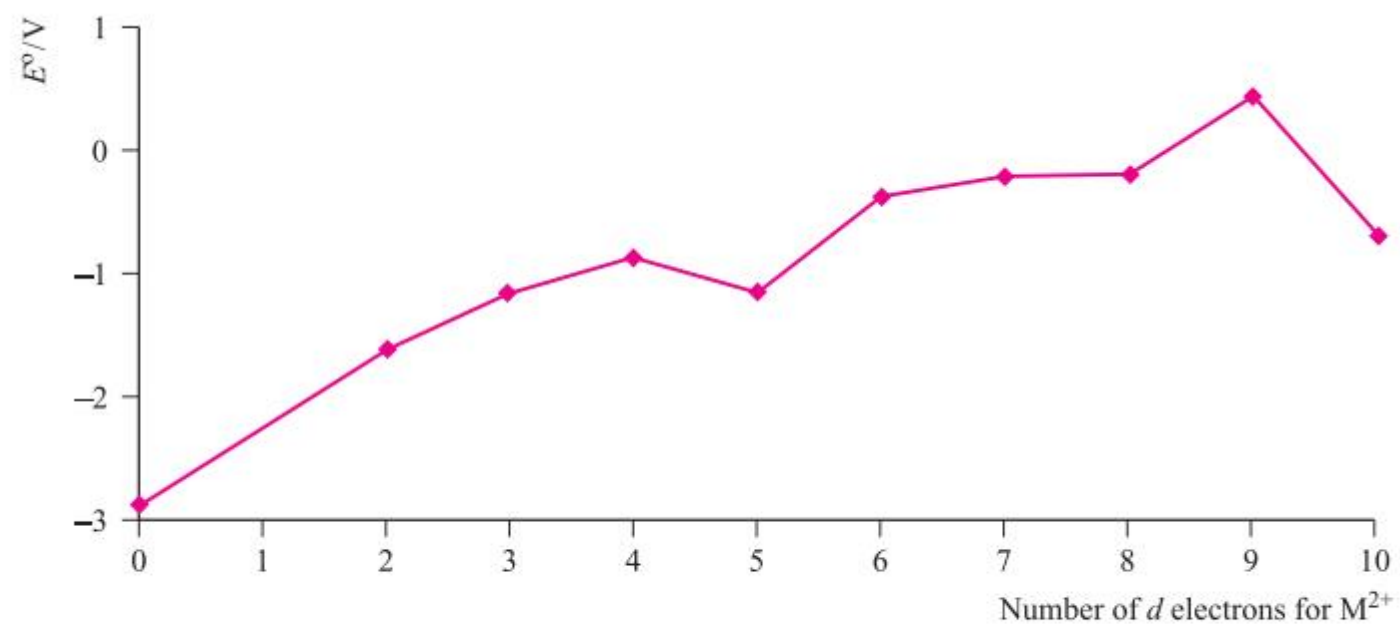
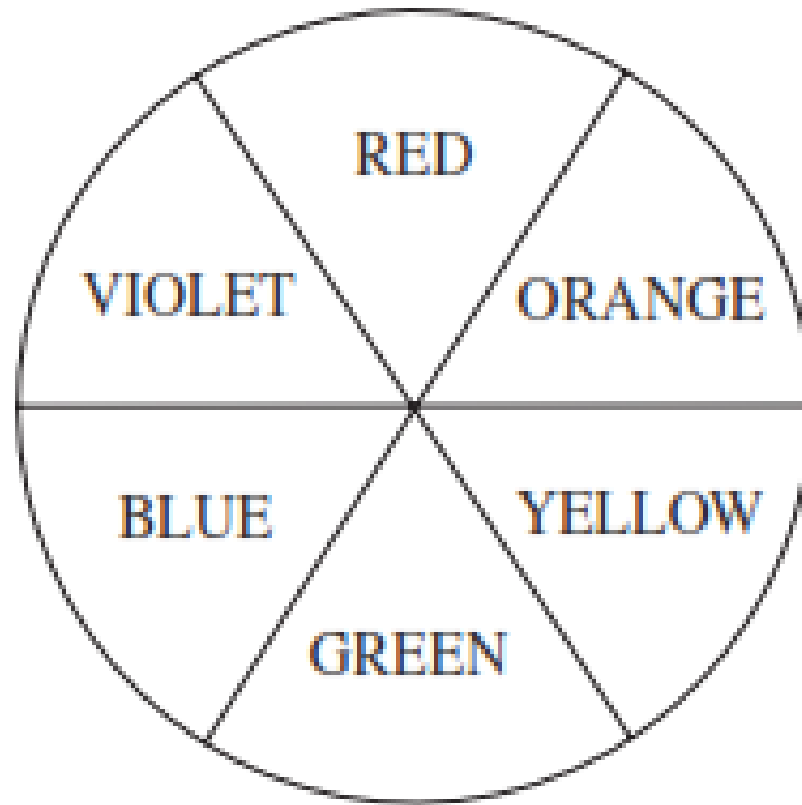
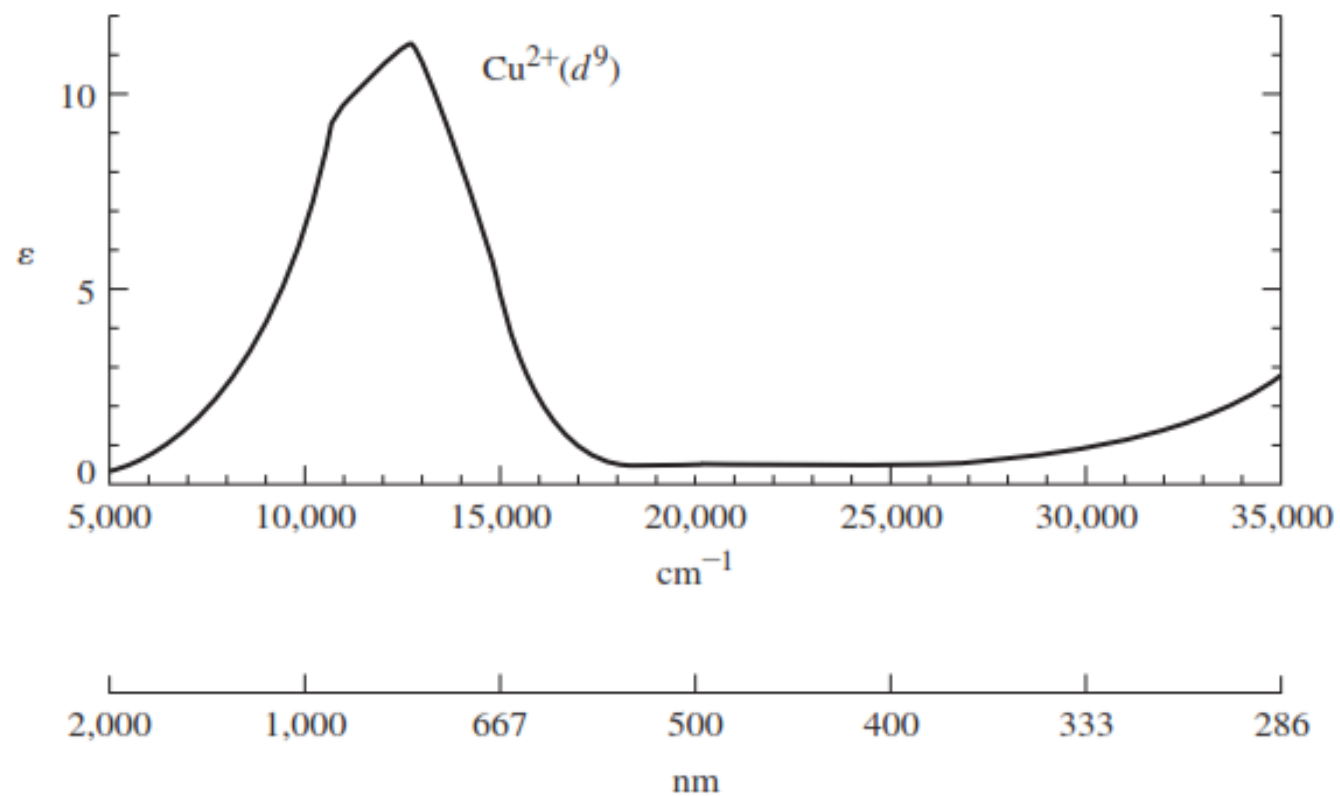


Fig. 20.30 The variation in values of $E^\circ(M^{2+}/M)$ as a function of d^n configuration for the first row metals; the point for d^0 corresponds to $M = \text{Ca}$.





$$\log \frac{I_o}{I} = A = \epsilon lc$$

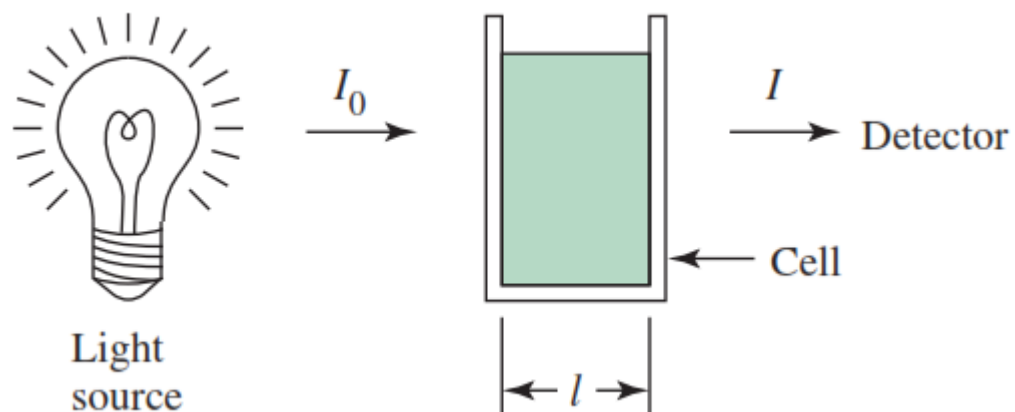


TABLE 11.1 Visible Light and Complementary Colors

Wavelength Range (nm)	Wave Numbers (cm ⁻¹)	Color	Complementary Color
< 400	> 25,000	Ultraviolet	
400–450	22,000–25,000	Violet	Yellow
450–490	20,000–22,000	Blue	Orange
490–550	18,000–20,000	Green	Red
550–580	17,000–18,000	Yellow	Violet
580–650	15,000–17,000	Orange	Blue
650–700	14,000–15,000	Red	Green
> 700	< 14,000	Infrared	

Consider again the example of the energy levels of a carbon atom. Carbon has the electron configuration $1s^2 2s^2 2p^2$. At first glance, we might expect the p electrons to be degenerate, and have the same energy. However, there are three major energy levels for the p^2 electrons, differing in energy by pairing and exchange energies (Π_c and Π_e). In addition, the lowest major energy level is split into three slightly different energies, for a total of five energy levels. As an alternative to the discussion presented in Section 2.2.3, each energy level can be described as a combination of the m_l and m_s values of the $2p$ electrons.

Independently, each of the $2p$ electrons could have any of six possible m_l, m_s combinations:

$n = 2, l = 1$	(quantum numbers defining $2p$ orbitals)
$m_l = +1, 0, \text{ or } -1$	(three possible values)
$m_s = +\frac{1}{2} \text{ or } -\frac{1}{2}$	(two possible values)

The $2p$ electrons are not independent of each other, however; the orbital angular momenta (characterized by m_l values) and the spin angular momenta (characterized by m_s values) of the $2p$ electrons interact in a manner called **Russell–Saunders coupling** or **LS coupling**.^{*} An oversimplified view is to consider an electron as a particle; its orbital motion and spin generate magnetic fields (a charge in motion generates a magnetic field) and these fields created by multiple electrons can interact. These interactions produce atomic states called **microstates** that can be described by new quantum numbers:

$$\begin{array}{ll} M_L = \sum m_l & \text{Total orbital angular momentum} \\ M_S = \sum m_s & \text{Total spin angular momentum} \end{array}$$

an electron having $m_l = +1$ and $m_s = +\frac{1}{2}$ will be written as 1^+ .

One possible set of values for the two electrons in the p^2 configuration would be

$$\left. \begin{array}{lll} \text{First electron:} & m_l = +1 & \text{and } m_s = +\frac{1}{2} \\ \text{Second electron:} & m_l = 0 & \text{and } m_s = -\frac{1}{2} \end{array} \right\} \text{Notation: } 1^+0^-$$

TABLE 11.2 Microstate Table for p^2

		M_S		
		-1	0	+1
M_L	+2		$1^+ 1^-$	
	+1	$1^- 0^-$	$1^+ 0^-$ $1^- 0^+$	$1^+ 0^+$
	0	$-1^- 1^-$	$-1^+ 1^-$ $0^+ 0^-$ $-1^- 1^+$	$-1^+ 1^+$
	-1	$-1^- 0^-$	$-1^+ 0^-$ $-1^- 0^+$	$-1^+ 0^+$
	-2		$-1^+ -1^-$	

*The number of microstates = $i!/[j!(i-j)!]$, where i = number of m_l, m_s combinations (six here, because m_l can have values of 1, 0, and -1, and m_s can have values of $+\frac{1}{2}$ and $-\frac{1}{2}$) and j = number of electrons.

Determine the possible microstates for an s^1p^1 configuration, and use them to prepare a microstate table.

11

The s electron can have $m_l = 0$ and $m_s = \pm \frac{1}{2}$.

The p electron can have $m_l = +1, 0, -1$ and $m_s = \pm \frac{1}{2}$.

		M_S		
		-1	0	$+1$
M_L	$+1$	$0^- 1^-$	$0^- 1^+$ $0^+ 1^-$	$0^+ 1^+$
	0	$0^- 0^-$	$0^+ 0^-$ $0^- 0^+$	$0^+ 0^+$
	-1	$0^- -1^-$	$0^- -1^+$ $0^+ -1^-$	$0^+ -1^+$

The quantum numbers that describe states of multielectron atoms are defined as follows:

L = total orbital angular momentum quantum number

S = total spin angular momentum quantum number

J = total angular momentum quantum number

Atomic States	Individual Electrons
$M_L = 0, \pm 1, \pm 2, \dots, \pm L$	$m_l = 0, \pm 1, \pm 2, \dots, \pm l$
$M_S = S, S-1, S-2, \dots, -S$	$m_s = +\frac{1}{2}, -\frac{1}{2}$

$L = 0$	S state
$L = 1$	P state
$L = 2$	D state
$L = 3$	F state

Atomic states characterized by S and L are often called **free-ion terms** (sometimes Russell–Saunders terms) because they describe individual atoms or ions, free of ligands. Their labels are often called **term symbols**.^{**} Term symbols are composed of a letter relating to the value of L and a left superscript for the spin multiplicity. For example, the term symbol 3D corresponds to a state in which $L = 2$ and the spin multiplicity ($2S + 1$) is 3; 5F marks a state in which $L = 3$ and $2S + 1 = 5$.

Examples of Atomic States (Free-Ion Terms) and Quantum Numbers

Term	L	S
1S	0	0
2S	0	$\frac{1}{2}$
3P	1	1
4D	2	$\frac{3}{2}$
5F	3	2

1S (singlet S)

An S term has $L = 0$ and must therefore have $M_L = 0$. The spin multiplicity (the superscript) is $2S + 1$. Because $2S + 1 = 1$, S must equal 0 (and $M_S = 0$). There can be only one microstate having $M_L = 0$ and $M_S = 0$ for a 1S term. For the minimum configuration of two electrons we have the following:

$$\begin{array}{cc}
 & M_S \\
 & \begin{array}{|c|} \hline 0 \\ \hline \end{array} \\
 M_L & \begin{array}{|c|c|} \hline 0 & 0^+0^- \\ \hline \end{array}
 \end{array}
 \quad \text{or} \quad
 \begin{array}{cc}
 & M_S \\
 & \begin{array}{|c|} \hline 0 \\ \hline \end{array} \\
 M_L & \begin{array}{|c|c|} \hline 0 & x \\ \hline \end{array}
 \end{array}$$

Each microstate is designated by x in the second form of the table.

2P (doublet P)

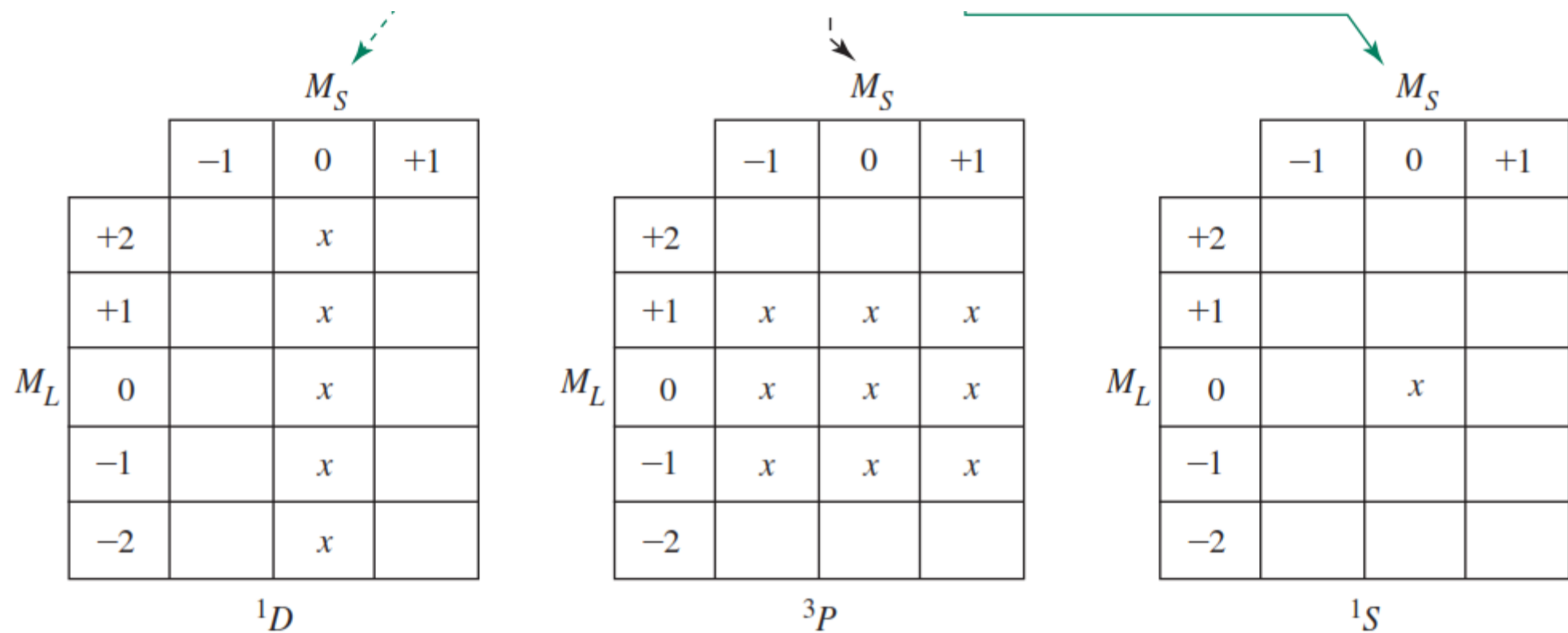
A P term has $L = 1$; therefore, M_L can have three values: $+1$, 0 , and -1 . The spin multiplicity is $2 = 2S + 1$. Therefore, $S = \frac{1}{2}$, and M_S can have two values: $+\frac{1}{2}$ and $-\frac{1}{2}$. There are six microstates in a 2P term ($3 \text{ rows} \times 2 \text{ columns}$). For the minimum case of one electron we have the following:

		M_S	
		$-\frac{1}{2}$	$+\frac{1}{2}$
M_L	1	1^-	1^+
	0	0^-	0^+
	-1	-1^-	-1^+

or

		M_S	
		$-\frac{1}{2}$	$+\frac{1}{2}$
M_L	1	x	x
	0	x	x
	-1	x	x

		M_S		
		-1	0	+1
M_L	+2		x	
	+1	x	x	x
	0	x	x	x
	-1	x	x	x
	-2		x	



Therefore, the p^2 electron configuration gives rise to three free-ion terms, designated 3P , 1D , and 1S . These terms have different energies; they represent three states with different degrees of electron–electron interactions. For our example of a p^2 configuration for a carbon atom, the 3P , 1D , and 1S terms have three distinct energies—the three major energy levels observed experimentally.

M_L	M_S	
	-1	0
		+1
+4		$(2^+, 2^-)$
+3	$(2^-, 1^-)$	$(2^+, 1^-)(2^-, 1^+)$
+2	$(2^-, 0^-)$	$(2^+, 0^-)(2^-, 0^+)(1^+, 1^-)$
+1	$(2^-, -1^-)(1^-, 0^-)$	$(2^+, -1^-)(2^-, -1^+)$
		$(1^+, 0^-)(1^-, 0^+)$
0	$(1^-, -1^-)(2^-, -2^-)$	$(1^+, -1^-)(1^-, -1^+)$
		$(2^+, -2^-)(2^-, -2^+)$
		$(0^+, 0^-)$
-1 to -4*		

* The lower half of the table is a reflection of the upper half.

The final step in this procedure is to determine which term has the lowest energy by using two of **Hund's rules**:

1. The ground term (term of lowest energy) has the highest spin multiplicity.
In our example of p^2 , the ground term is the 3P . This term can be identified as having the configuration in the margin. This is sometimes called *Hund's rule of maximum multiplicity*, introduced in Section 2.2.3.
2. If two or more terms share the maximum spin multiplicity, the ground term is the one having the highest value of L .
For example, if 4P and 4F terms are both found for an electron configuration, the 4F has lower energy: 4F has $L = 3$, and 4P has $L = 1$.

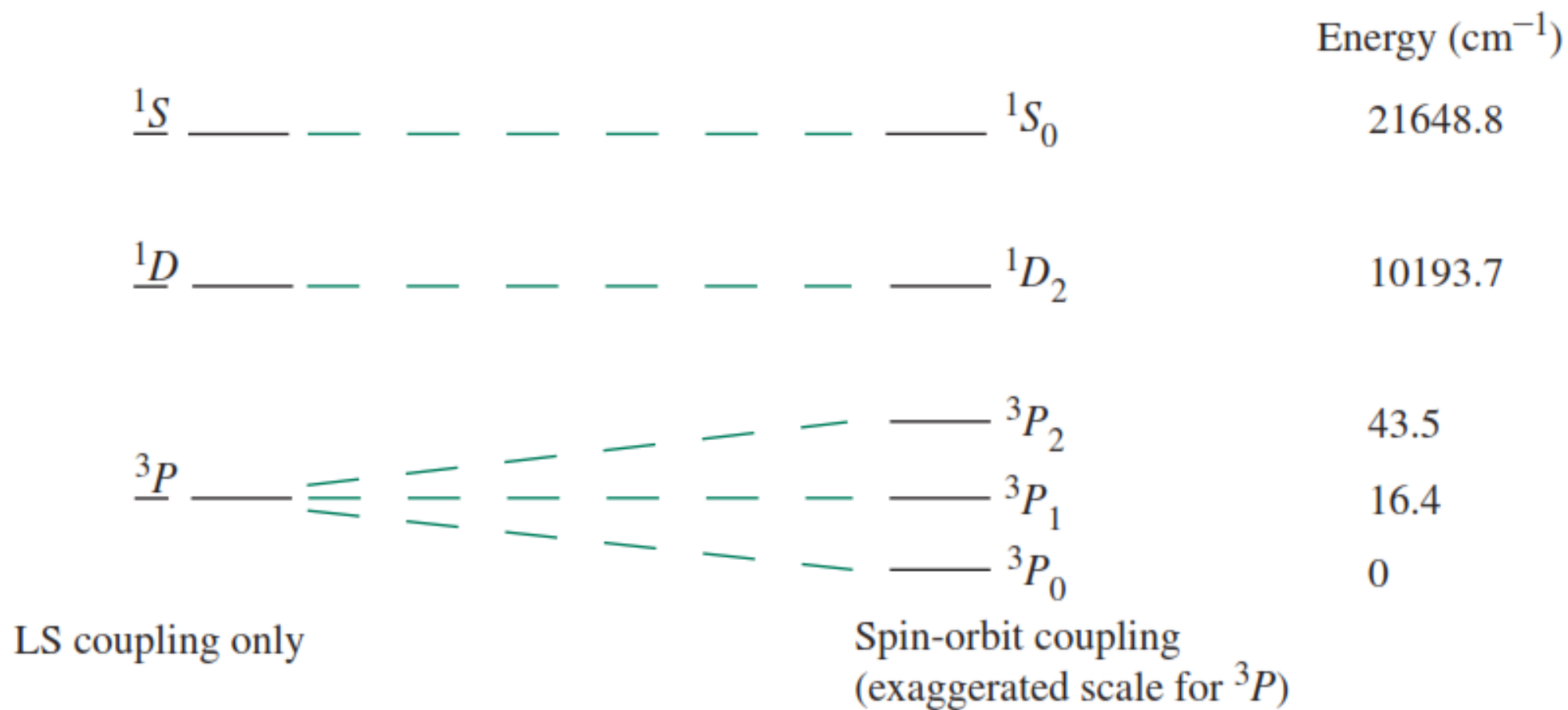
Spin-Orbit Coupling

Up to this point in the discussion of multielectron atoms, the spin and orbital angular momenta have been treated separately. An additional factor is important: the spin and orbital angular momenta (or the magnetic fields associated with them) couple with each other, a phenomenon known as *spin-orbit coupling*. In multielectron atoms, the S and L quantum numbers combine into the total angular momentum quantum number J . The quantum number J may have the following values:

$$J = L + S, L + S - 1, L + S - 2, \dots, |L - S|$$

Determine the possible values of J for the carbon terms.

For the term symbols just described for carbon, the 1D and 1S terms each have only one J value, whereas the 3P term has three slightly different energies, each described by a different J . J can have only the value 0 for the 1S term ($0 + 0$) and only the value 2 for the 1D term ($2 + 0$). For the 3P term, J can have the three values 2, 1, and 0 ($1 + 1$, $1 + 1 - 1$, and $1 + 1 - 2$).



These are the five energy states for the carbon atom referred to at the beginning of this section. The state of lowest energy (spin-orbit coupling included) can be predicted from **Hund's third rule**:

3. For subshells (such as p^2) that are less than half filled, the state having the lowest J value has the lowest energy (3P_0 for p^2); for subshells that are more than half filled, the state having the highest J value has the lowest energy. Half-filled subshells have only one possible J value.

TABLE 11.5 Free-Ion Terms for d^n Configurations

Configuration	Free-Ion Terms						
d^1	2D						
d^2		$^1S^1D^1G$	$^3P^3F$				
d^3	2D		$^4P^4F$	$^2P^2D^2F^2G^2H$			
d^4	5D	$^1S^1D^1G$	$^3P^3F$	$^3P^3D^3F^3G^3H$	$^1S^1D^1F^1G^1I$		
d^5	2D		$^4P^4F$	$^2P^2D^2F^2G^2H$	$^2S^2D^2F^2G^2I$	$^4D^4G$	6S
d^6	Same as d^4						
d^7	Same as d^3						
d^8	Same as d^2						
d^9	Same as d^1						
d^{10}	1S						

In the interpretation of spectra of coordination compounds, it is often important to identify the lowest-energy term. A quick and fairly simple way to do this is given here, using as an example a d^3 configuration in octahedral symmetry.*

1. Sketch the energy levels, showing the d electrons.



2. Spin multiplicity of lowest-energy state = number of unpaired electrons + 1.**

$$\text{Spin multiplicity} = 3 + 1 = 4$$

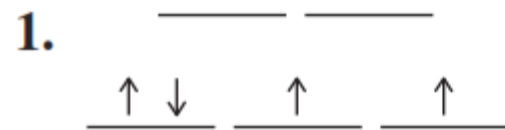
3. Determine the maximum possible value of M_L (sum of m_l values) for the configuration as shown. This determines the type of free-ion term (e.g., S , P , D).

Maximum possible value of M_L for three electrons as shown: $2 + 1 + 0 = 3$; therefore, F term

4. Combine results of Steps 2 and 3 to get the ground term.

$4F$

What is the ground term for d^4 (low spin)?



2. Spin multiplicity = $2 + 1 = 3$

3. Highest possible value of $M_L = 2 + 2 + 1 + 0 = 5$; therefore, H term.

Note that here, $m_l = 2$ for the first two electrons does not violate the exclusion principle because the electrons have opposite spins.

4. Therefore, the ground term is 3H .

Selection Rules

1. Transitions between states of the same parity (symmetry with respect to a center of inversion) are forbidden. For example, transitions between states that arise from d orbitals are forbidden ($g \longrightarrow g$ transitions; d orbitals are symmetric to inversion), but transitions between states arising from d and p orbitals are allowed ($g \longrightarrow u$ transitions; p orbitals are antisymmetric to inversion). This is known as the **Laporte selection rule**.
2. Transitions between states of different spin multiplicities are forbidden. For example, transitions between 4A_2 and 4T_1 states are “spin-allowed,” but between 4A_2 and 2A_2 are “spin-forbidden.” This is called the **spin selection rule**.

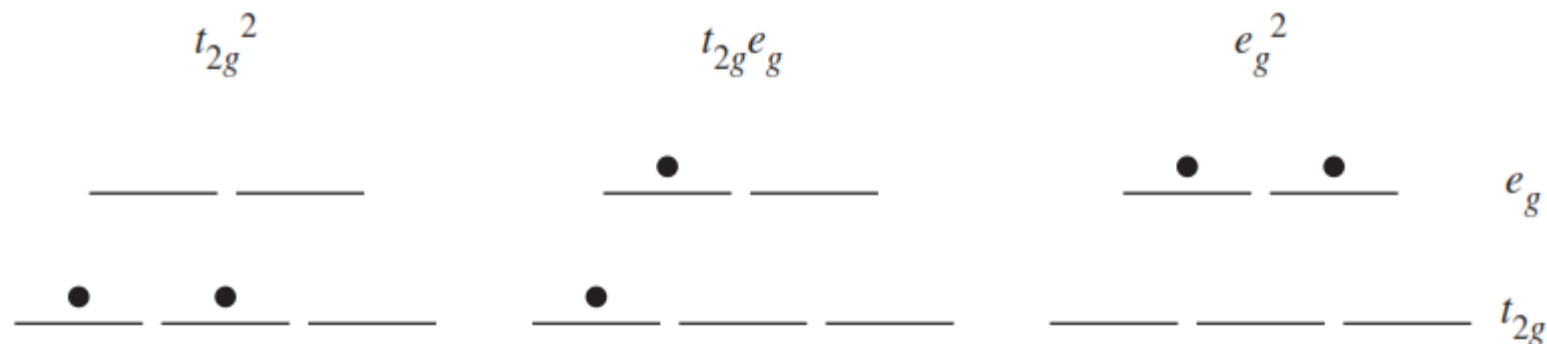
1. The bonds in transition-metal complexes, like all chemical bonds, undergo vibrations that may temporarily change the symmetry. Octahedral complexes, for example, vibrate in ways in which the center of symmetry is temporarily lost; this phenomenon, called *vibronic coupling*, can relax the first selection rule. As a consequence, $d-d$ transitions having molar absorptivities in the range of approximately $5-50 \text{ L mol}^{-1} \text{ cm}^{-1}$ commonly occur, and they are often responsible for the bright colors of these complexes.
2. Tetrahedral complexes often absorb more strongly than octahedral complexes of the same metal in the same oxidation state. Metal–ligand σ bonding in transition-metal complexes of T_d symmetry can be described as involving a combination of sp^3 and sd^3 hybridization of the metal orbitals; both types of hybridization are consistent with the symmetry. The mixing of p -orbital character (of u symmetry) with d -orbital character provides a second way of relaxing the first selection rule.

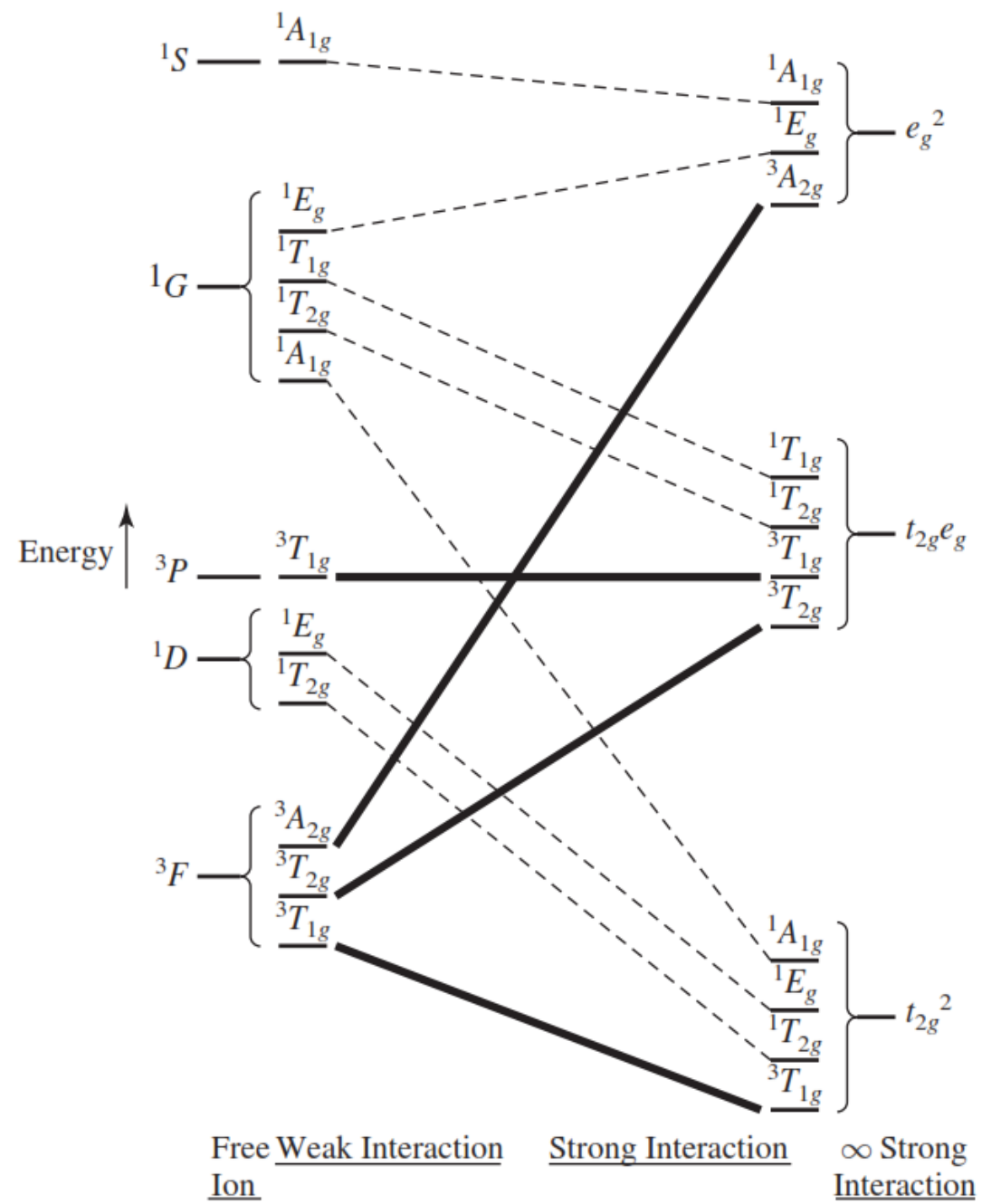
3. Spin-orbit coupling in some cases provides a mechanism of relaxing the second selection rule, with the result that transitions may be observed from a ground state of one spin multiplicity to an excited state of different spin multiplicity. Such absorption bands for first-row transition-metal complexes are usually very weak, with typical molar absorptivities less than $1 \text{ L mol}^{-1} \text{ cm}^{-1}$. For complexes of second- and third-row transition metals, spin-orbit coupling can be more important.

In discussing spectra, it will be particularly useful to relate the electronic spectra of transition-metal complexes to the ligand field splitting, Δ_o , for octahedral complexes. To do this it will be necessary to introduce **correlation diagrams** and **Tanabe–Sugano diagrams**.

1. Free ions (no ligand field). In Exercise 11.4, the terms 3F , 3P , 1G , 1D , and 1S were obtained for a d^2 configuration, with the 3F term having the lowest energy. These terms describe the energy levels of a “free” d^2 ion—in our example, a V^{3+} ion—in the absence of any interactions with ligands. In correlation diagrams, we will show these free-ion terms on the far left.

2. Strong ligand field. There are three possible configurations for two d electrons in an octahedral ligand field:





1. The free-ion states (terms arising from LS coupling) are shown on the far left.
2. The extremely strong field states are shown on the far right.

TABLE 11.6 Splitting of Free-Ion Terms in Octahedral Symmetry

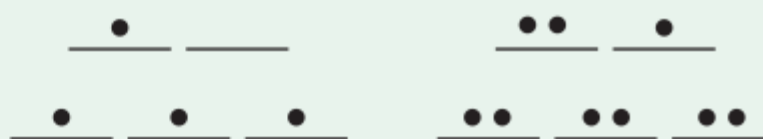
Term	Irreducible Representations
S	A_{1g}
P	T_{1g}
D	$E_g + T_{2g}$
F	$A_{2g} + T_{1g} + T_{2g}$
G	$A_{1g} + E_g + T_{1g} + T_{2g}$
H	$E_g + 2T_{1g} + T_{2g}$
I	$A_{1g} + A_{2g} + E_g + T_{1g} + 2T_{2g}$

Examples

T Designates a triply degenerate asymmetrically occupied state.



E Designates a doubly degenerate asymmetrically occupied state.

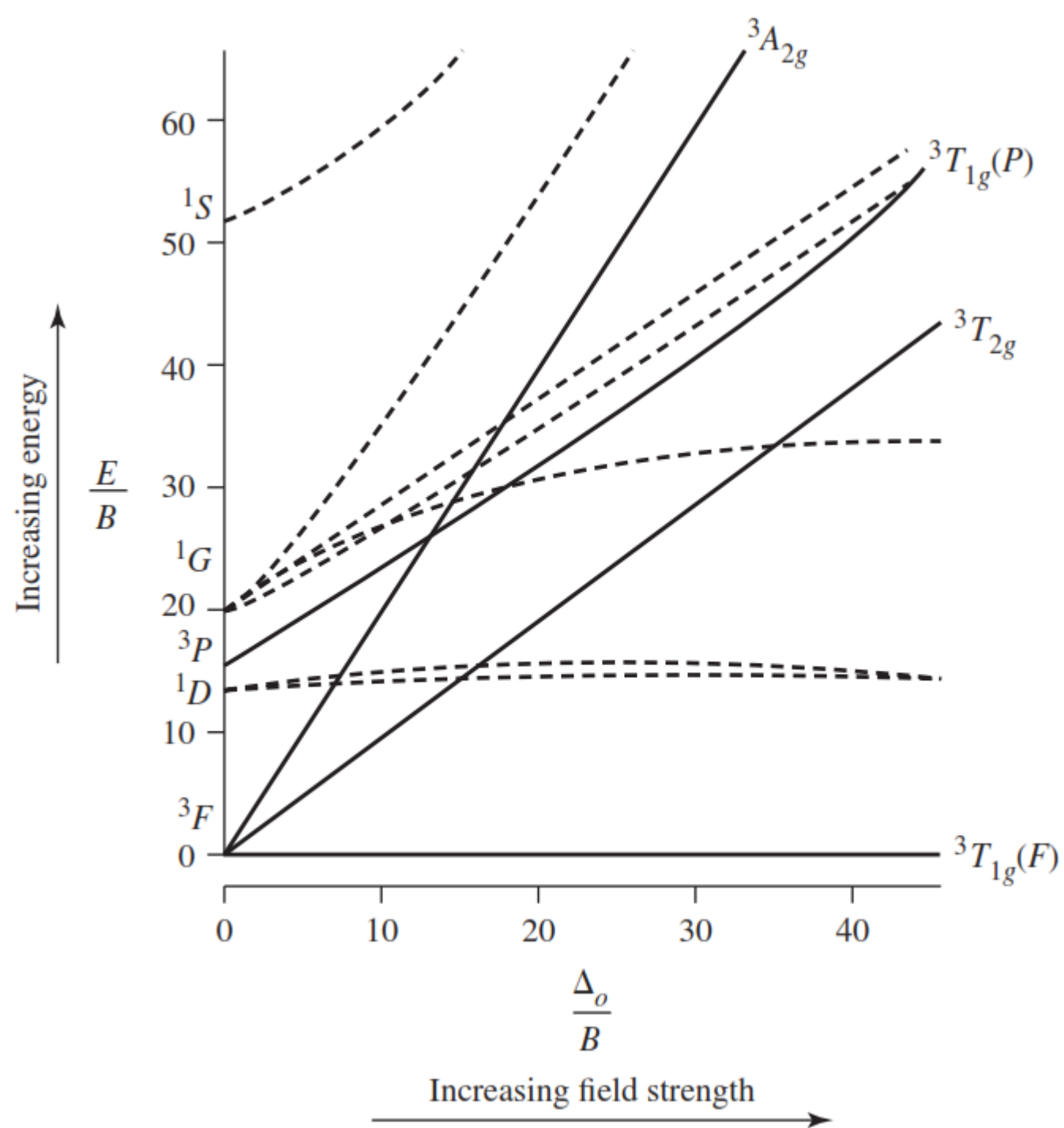


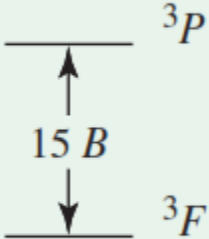
A or *B* Designate a nondegenerate state. Each set of levels in an *A* or *B* state is symmetrically occupied.



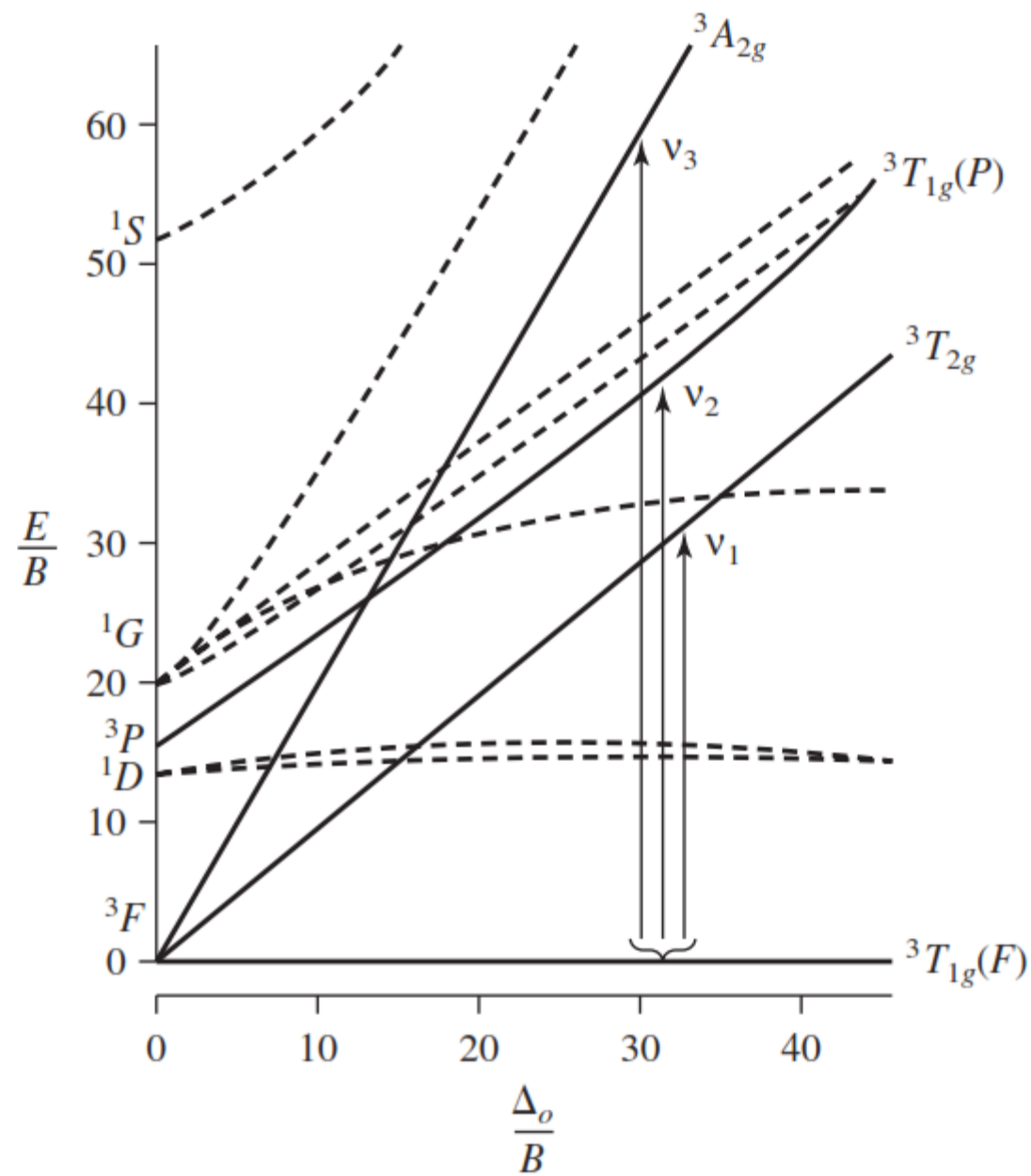
Tanabe–Sugano Diagrams

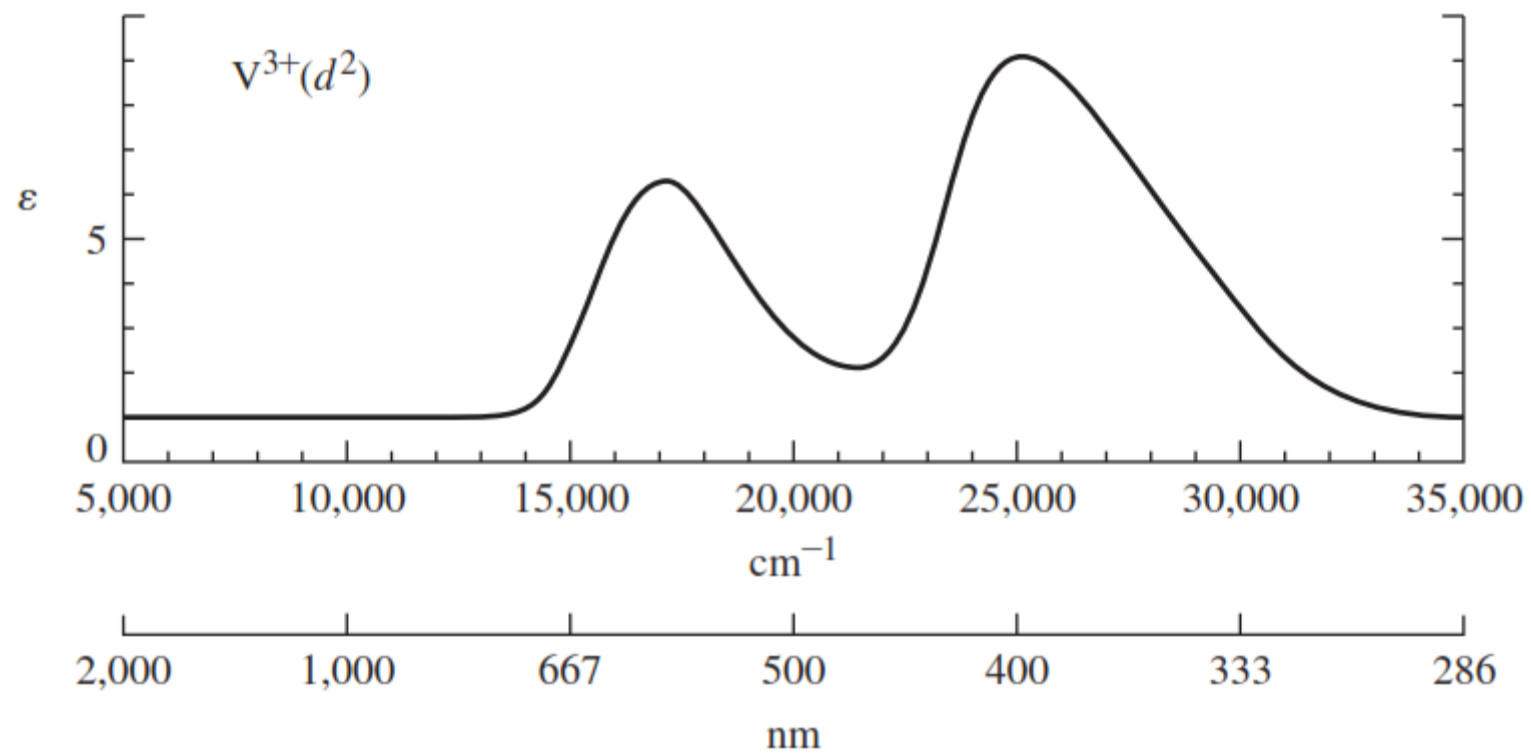
Tanabe–Sugano diagrams are modified correlation diagrams that are useful in the interpretation of electronic spectra of coordination compounds.⁵ In Tanabe–Sugano diagrams, the lowest-energy state is plotted along the horizontal axis; consequently, the vertical distance above this axis is a measure of the energy of the excited state above the ground state. For example, for the d^2 configuration, the lowest-energy state is described by the line in the correlation diagram (Figure 11.3) joining the ${}^3T_{1g}$ state arising from the 3F free-ion term with the ${}^3T_{1g}$ state arising from the strong-field term, t_{2g}^2 . In the Tanabe–Sugano diagram (**Figure 11.4**), this line is made horizontal*; it is labeled ${}^3T_{1g} (F)$ and is shown to arise from the 3F term in the free-ion limit (left side of diagram).**

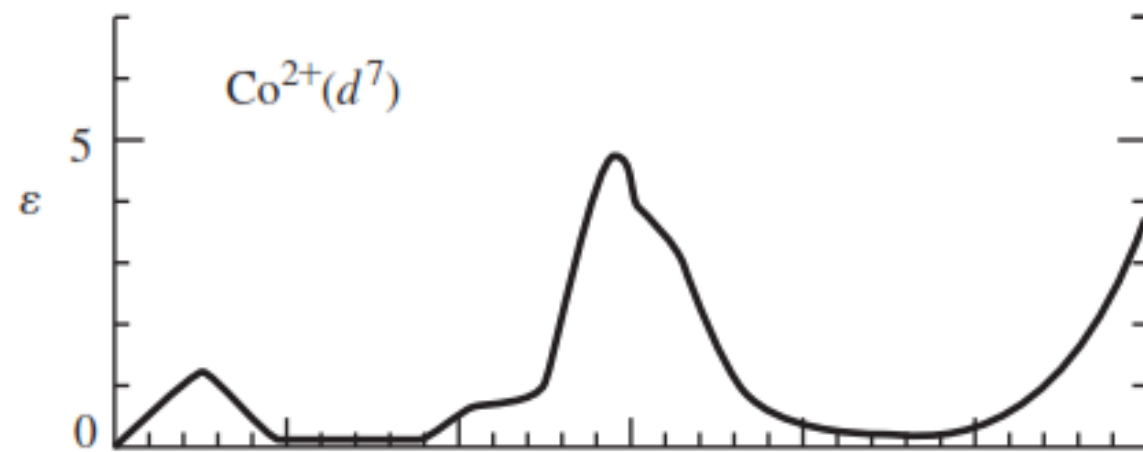
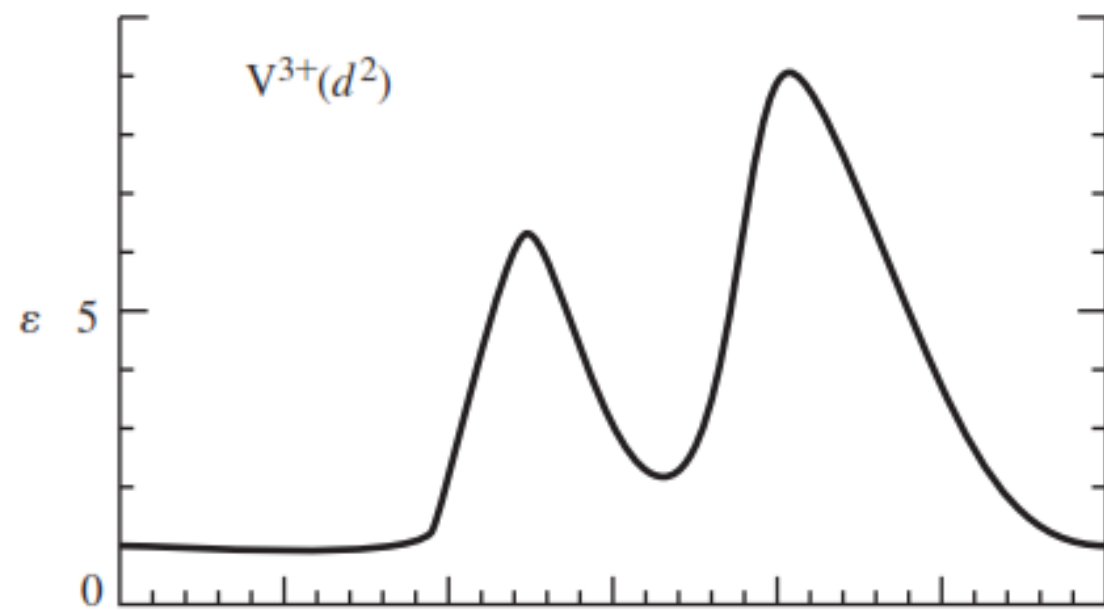
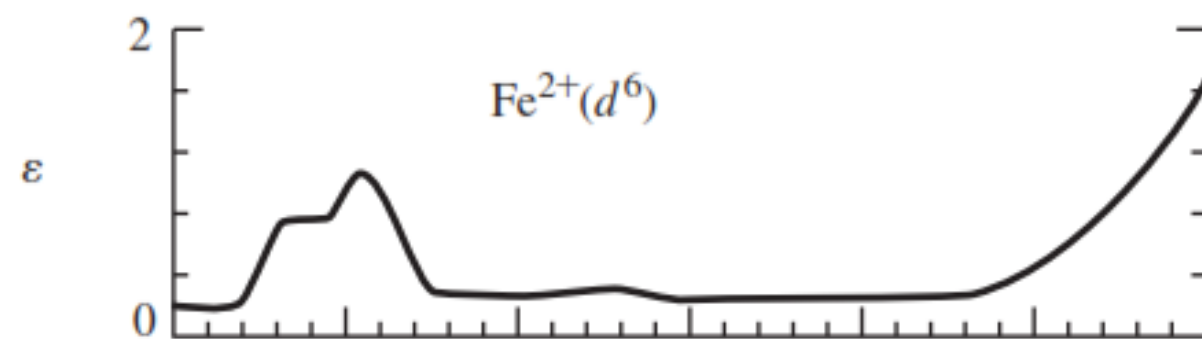
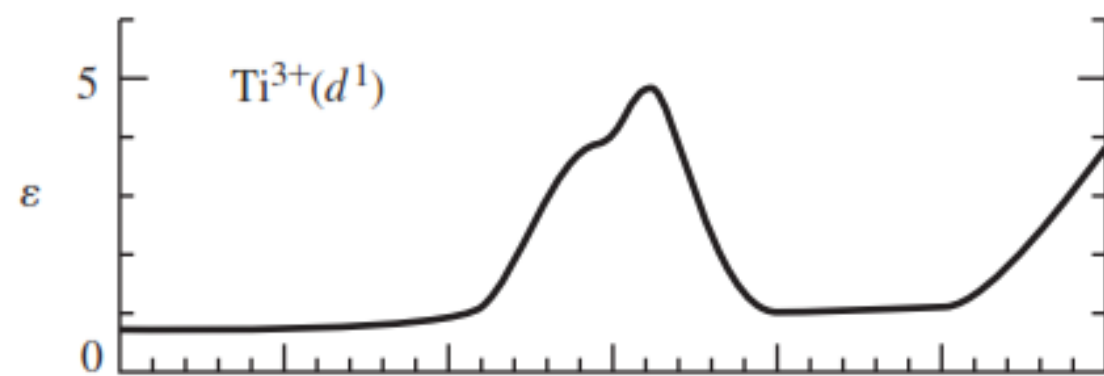


<i>Horizontal axis:</i>	$\frac{\Delta_o}{B}$	where Δ_o is the octahedral ligand field splitting, described in Chapter 10.
	$B =$	Racah parameter, a measure of the repulsion between terms of the same multiplicity. For d^2 , for example, the energy difference between 3F and 3P is $15B$.
<i>Vertical axis:</i>	$\frac{E}{B}$	where E is the energy (of excited states) above the ground state.

$$\begin{aligned} \nu_1: {}^3T_{1g}(F) &\rightarrow {}^3T_{2g} \\ \nu_2: {}^3T_{1g}(F) &\rightarrow {}^3T_{1g}(P) \\ \nu_3: {}^3T_{1g}(F) &\rightarrow {}^3A_{2g} \end{aligned}$$

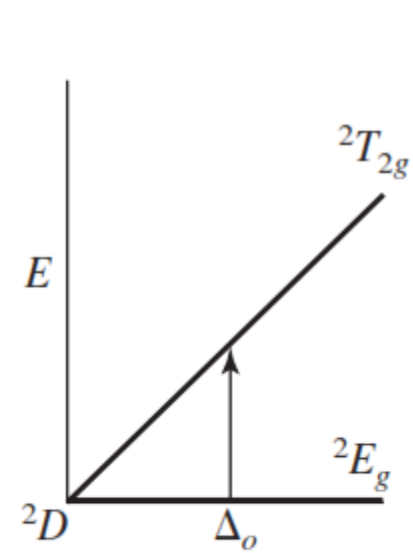
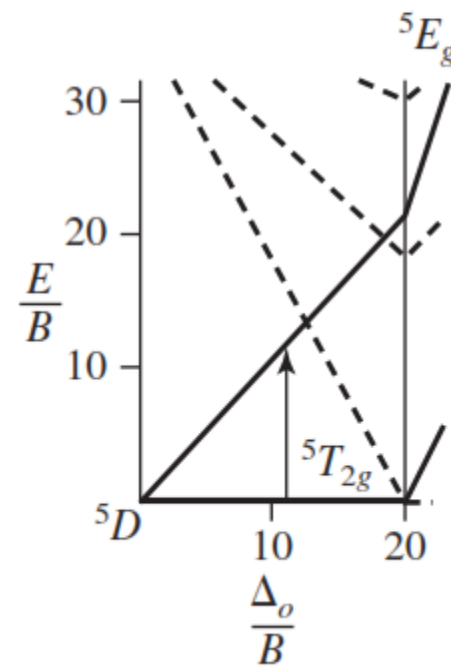
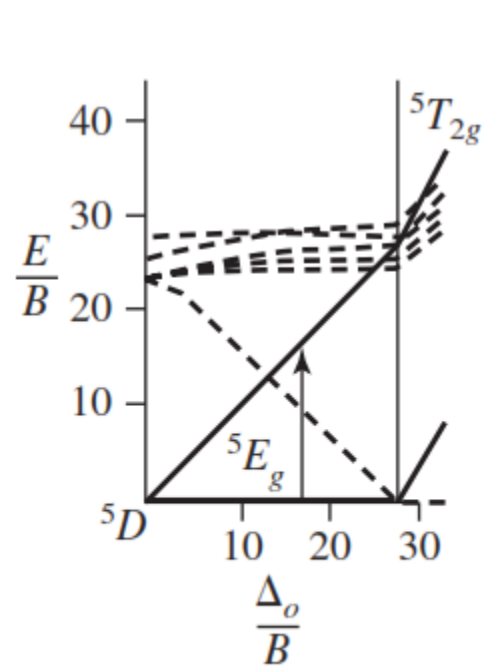
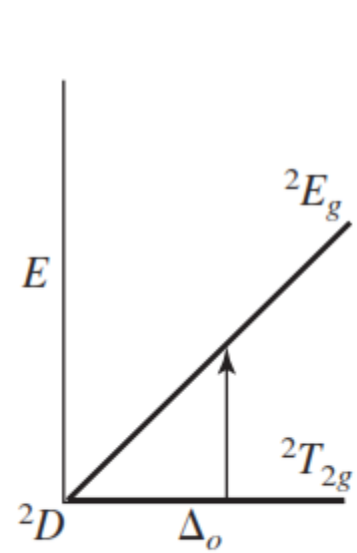
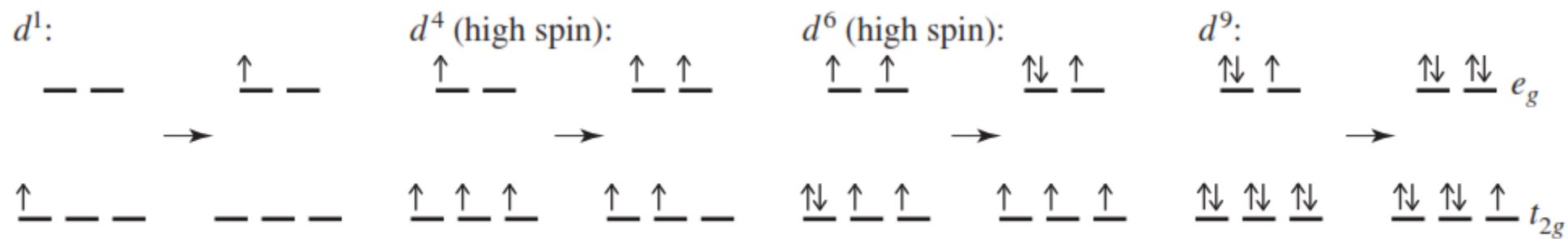






d^1 , d^4 (High Spin), d^6 (High Spin), d^9

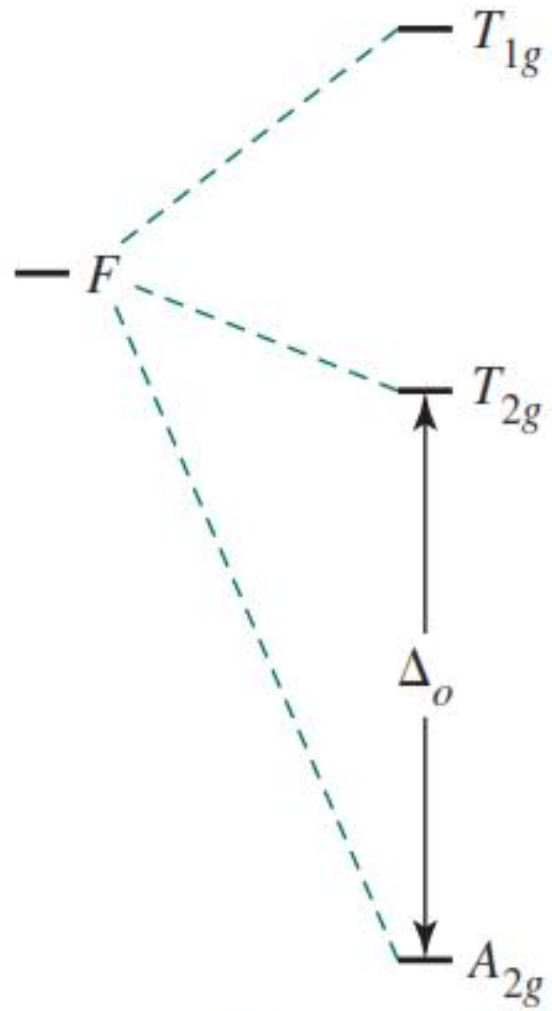
From a simple perspective each of these cases in **Figure 11.11** corresponds to excitation of an electron from a t_{2g} to an e_g orbital, with the final (excited) electron configuration having the same spin multiplicity as the initial configuration. Our discussion in this chapter indicates that when electron–electron interactions are considered there is a single excited state of the same spin multiplicity as the ground state for each of these configurations. Consequently, there is a single spin-allowed absorption, with the energy of the absorbed light equal to Δ_o . Examples of such complexes include $[\text{Ti}(\text{H}_2\text{O})_6]^{3+}$, $[\text{Cr}(\text{H}_2\text{O})_6]^{2+}$, $[\text{Fe}(\text{H}_2\text{O})_6]^{2+}$, and $[\text{Cu}(\text{H}_2\text{O})_6]^{2+}$; note from Figure 11.8 that each of these complexes exhibits essentially a single absorption band. In some cases, splitting of bands due to Jahn–Teller distortion is observed (Section 11.3.4).



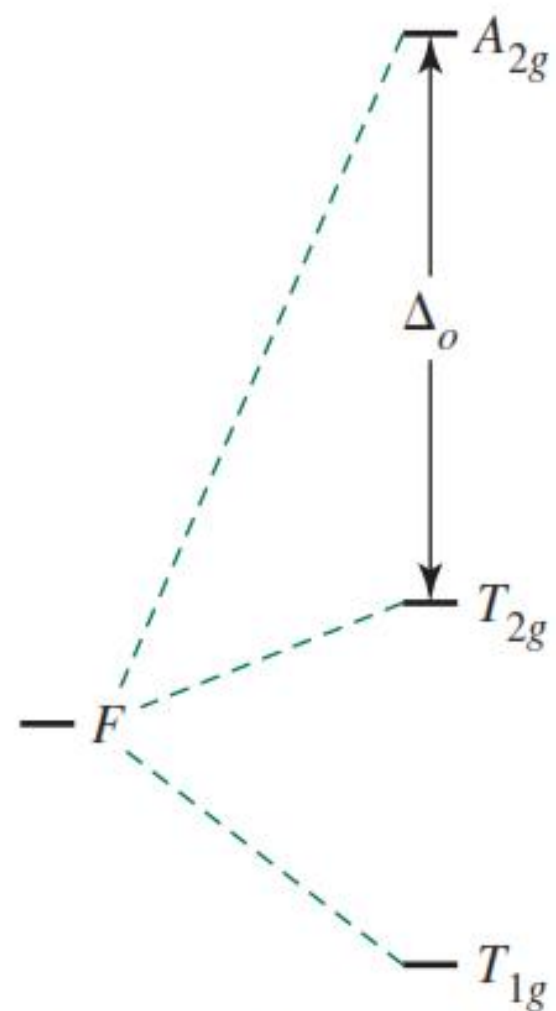
d^3, d^8

These electron configurations have a ground-state F term. In an octahedral ligand field, an F term splits into three terms: A_{2g} , T_{2g} , and T_{1g} . As shown in **Figure 11.12**, the A_{2g} is of lowest energy for d^3 or d^8 . For these configurations, the difference in energy between the two lowest-energy terms, the A_{2g} and the T_{2g} , is equal to Δ_o . Therefore, to approximate

Δ_o , we determine the energy of the band associated with the A_{2g} to T_{2g} transition, which is typically the lowest energy absorption in the electronic spectrum. Examples include $[\text{Cr}(\text{H}_2\text{O})_6]^{3+}$ and $[\text{Ni}(\text{H}_2\text{O})_6]^{2+}$. In these complexes, the lowest-energy band in the spectra (Figure 11.8) is for the transition from the $^4A_{2g}$ ground state to the $^4T_{2g}$ excited state. The energies of these bands, approximately 17,500 and 8,500 cm^{-1} , respectively, are the values of Δ_o .



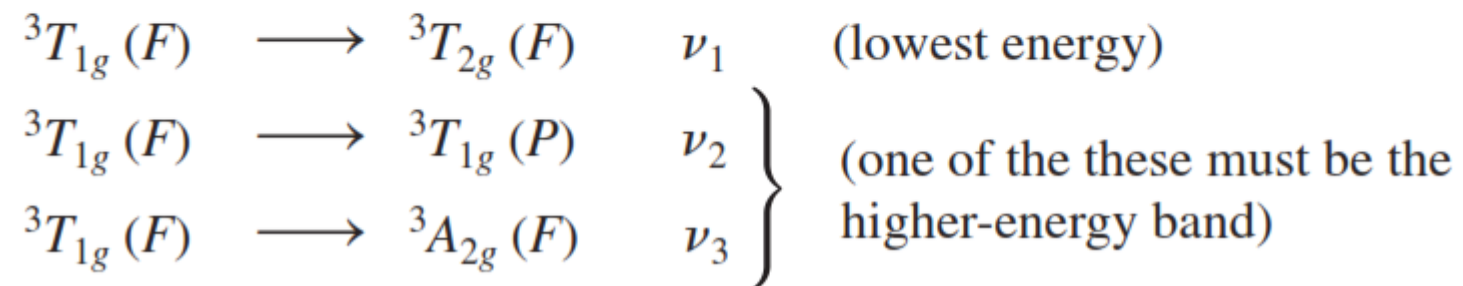
d^3 (or d^8) Configuration



d^2 (or d^7) Configuration

$[\text{V}(\text{H}_2\text{O})_6]^{3+}$ has absorption bands at $17,800$ and $25,700 \text{ cm}^{-1}$. Using the Tanabe–Sugano diagram for d^2 , estimate values of Δ_o and B for this complex.

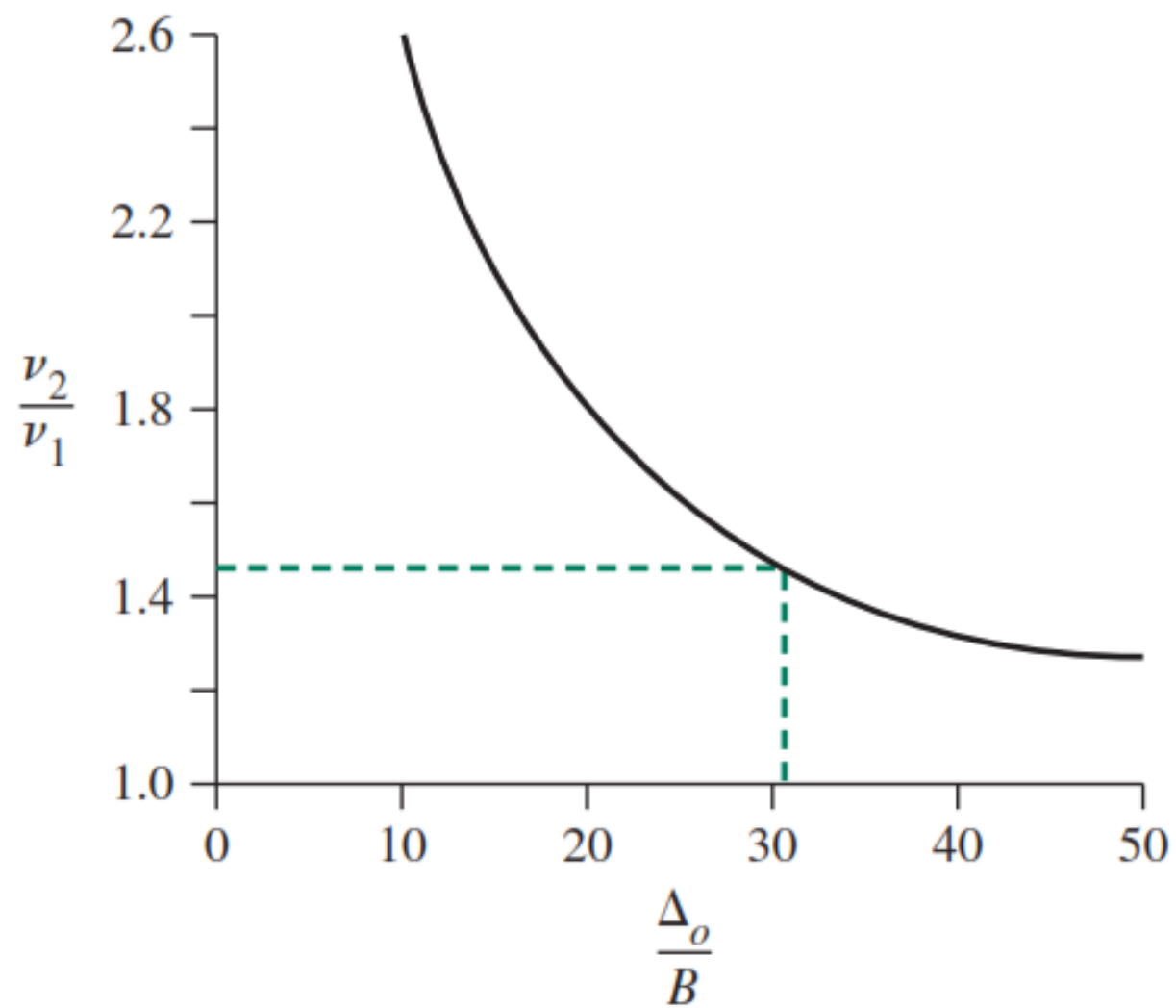
From the Tanabe–Sugano diagram there are three possible spin-allowed transitions (Figure 11.13):



It is often useful to determine the ratio of energies of the absorption bands. In this example,

$$\frac{25,700 \text{ cm}^{-1}}{17,800 \text{ cm}^{-1}} = 1.44$$

$\frac{\Delta_o}{B}$	E/B		$\frac{\nu_2}{\nu_1}$
	ν_1	ν_2	
0	0	15	—
10	8.74	21.5	2.46
20	18.2	31.4	1.73
30	27.9	40.8	1.46
40	37.7	50.4	1.34
50	47.6	60.2	1.26



The ratio ν_2 / ν_1 varies as a function of the strength of the ligand field. By plotting the ratio ν_2 / ν_1 versus Δ_o / B after extracting these values from the Tanabe–Sugano diagram (**Figure 11.14**), we find that $\nu_2 / \nu_1 = 1.44$ at approximately $\Delta_o / B = 31$.^{10,*}

$$\text{At } \frac{\Delta_o}{B} = 31,$$

$$\nu_2 : \frac{E}{B} = 42 \text{ (approximately); } B = \frac{E}{42} = \frac{25,700 \text{ cm}^{-1}}{42} = 610 \text{ cm}^{-1}$$

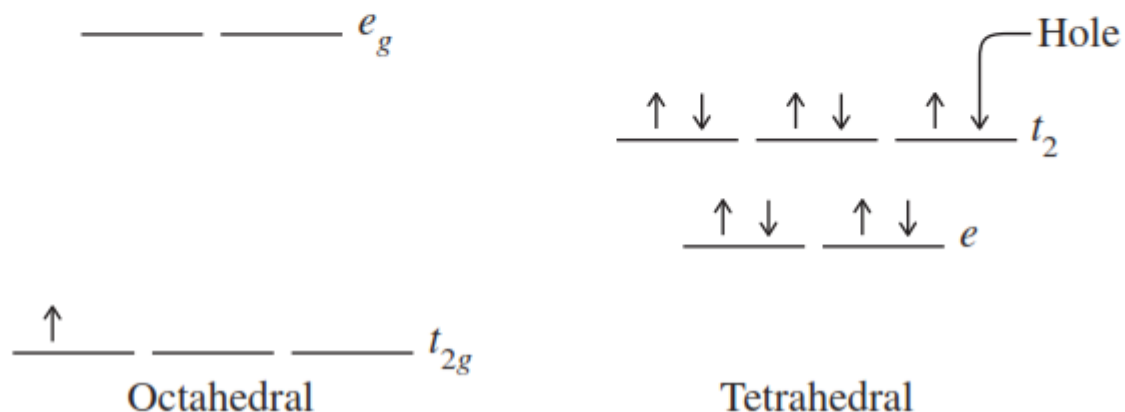
$$\nu_1 : \frac{E}{B} = 29 \text{ (approximately); } B = \frac{E}{29} = \frac{17,800 \text{ cm}^{-1}}{29} = 610 \text{ cm}^{-1}$$

$$\text{Because } \frac{\Delta_o}{B} = 31,$$

$$\Delta_o = 31 \times B = 31 \times 610 \text{ cm}^{-1} = 19,000 \text{ cm}^{-1}$$

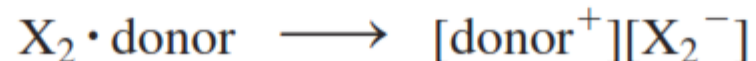
Tetrahedral Complexes

A useful comparison can be drawn between these by using the **hole formalism**. This is best illustrated by example. Consider a d^1 configuration in an octahedral complex. The one electron occupies an orbital in a triply degenerate set (t_{2g}). Now, consider a d^9 configuration in a tetrahedral complex. This configuration has a “hole” in a triply degenerate set of orbitals (t_2). It can be shown that, in terms of symmetry, the $d^1 O_h$ configuration is analogous to the $d^9 T_d$ configuration; the “hole” in d^9 results in the same symmetry as the single electron in d^1 .

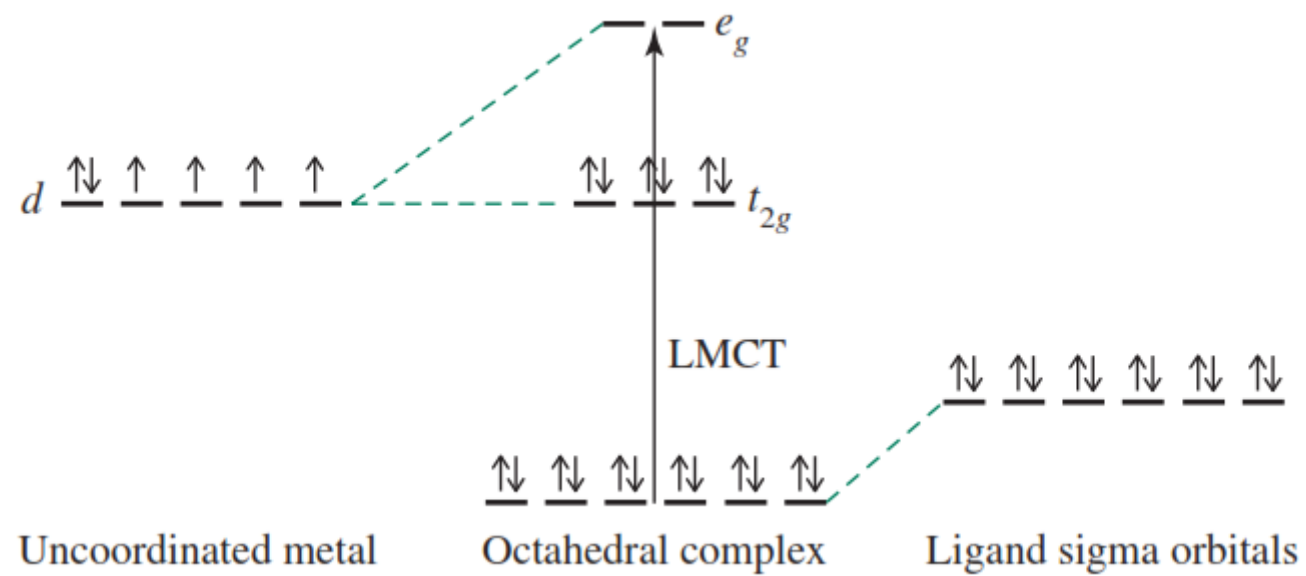


Charge-Transfer Spectra

Charge-transfer absorptions in solutions of halogens are described in Chapter 6. In these cases, a strong interaction between a donor solvent and a halogen molecule, X_2 , leads to the formation of a complex in which an excited state (primarily of X_2 character) can accept electrons from a HOMO (primarily of solvent character) on absorption of light of suitable energy:



Electrons can be excited, not only from the t_{2g} level to the e_g , but also from the σ orbitals originating from the ligands to the e_g . The latter excitation results in a charge-transfer transition, designated as **ligand to metal charge transfer (LMCT)** (also called charge transfer to metal, CTTM). This type of transition results in formal reduction of the metal. A LMCT excitation involving a cobalt (III) complex, for example, would exhibit an excited state having cobalt(II).

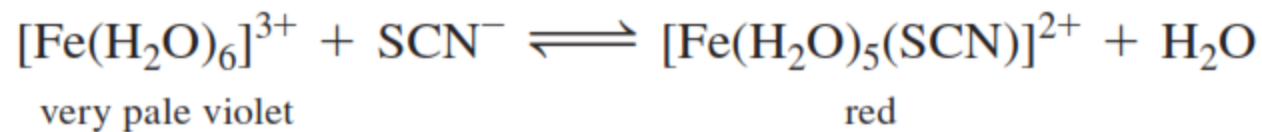
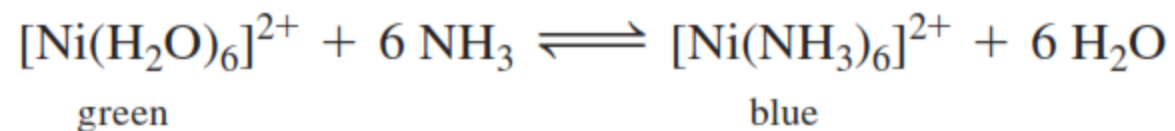


Similarly, it is possible for there to be **metal to ligand charge transfer (MLCT)** (also called charge transfer to ligand, CTTL) in coordination compounds having π -acceptor ligands. In these cases, empty π^* orbitals on the ligands become the acceptor orbitals on absorption of light. **Figure 11.16** illustrates this phenomenon for a d^5 complex, again from the oversimplified angular overlap perspective.

The isoelectronic ions VO_4^{3-} , CrO_4^{2-} , and MnO_4^- all have intense charge-transfer transitions. The wavelengths of these transitions increase in this series, with MnO_4^- having its charge-transfer absorption at the longest wavelength. Suggest a reason for this trend.

Substitution Reactions

Inert and Labile Compounds



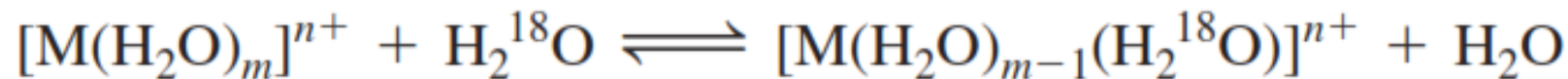
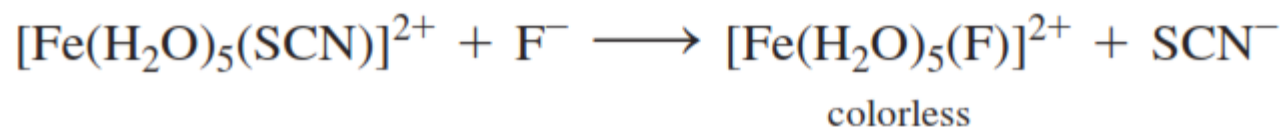
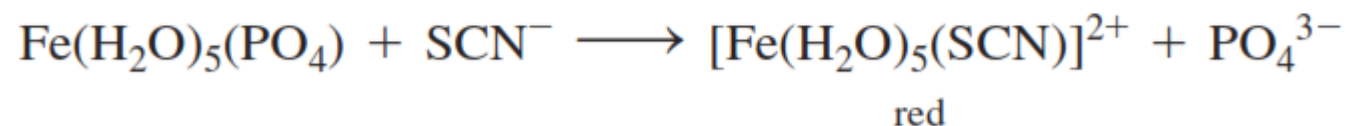
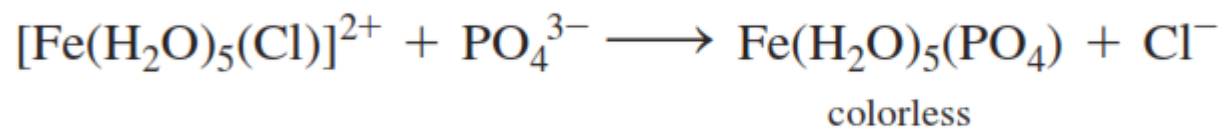
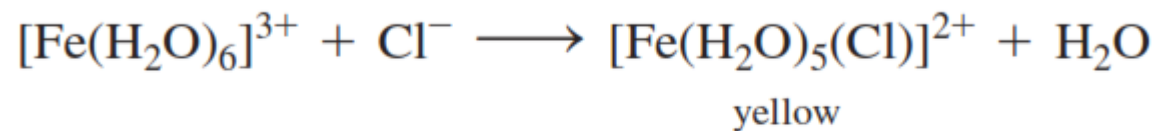
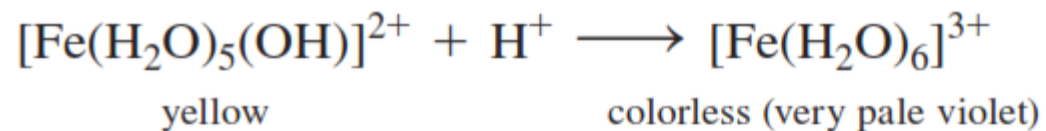


TABLE 12.1 Rate Constants for Water Exchange in $[M(H_2O)_6]^{n+}$

Complex	$k(s^{-1})$ (298 K)	Electronic Configuration*
$[Ti(H_2O)_6]^{3+}$	1.8×10^5	t_{2g}^1
$[V(H_2O)_6]^{3+}$	5.0×10^2	t_{2g}^2
$[V(H_2O)_6]^{2+}$	8.7×10^1	t_{2g}^3
$[Cr(H_2O)_6]^{3+}$	2.4×10^{-6}	t_{2g}^3
$[Cr(H_2O)_6]^{2+}$	$> 10^8$	$t_{2g}^3 e_g^1$
$[Fe(H_2O)_6]^{3+}$	1.6×10^2	$t_{2g}^3 e_g^2$
$[Fe(H_2O)_6]^{2+}$	4.4×10^6	$t_{2g}^4 e_g^2$
$[Co(H_2O)_6]^{2+}$	3.2×10^6	$t_{2g}^5 e_g^2$
$[Ni(H_2O)_6]^{2+}$	3.2×10^4	$t_{2g}^6 e_g^2$
$[Cu(H_2O)_6]^{2+}$	4.4×10^9	$t_{2g}^6 e_g^3$
$[Zn(H_2O)_6]^{2+}$	$> 10^7$	$t_{2g}^6 e_g^4$

Slow Reactions (Inert)

d^3 , low-spin d^4 , d^5 , and d^6

Strong-field d^8 (square planar)

Moderate Rate

Weak-field d^8

Fast Reactions (Labile)

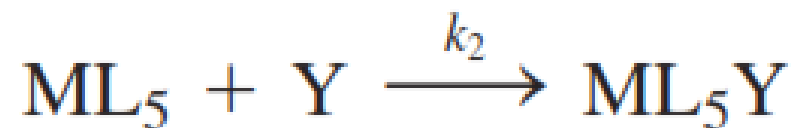
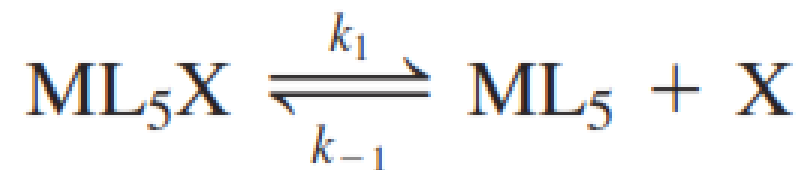
d^1 , d^2 , high-spin d^4 , d^5 , and d^6

d^7 , d^9 , d^{10}

Mechanisms of Substitution

Langford and Gray² described a range of possibilities for substitution reactions (**Table 12.2**). At one extreme, the departing ligand leaves, and an intermediate with a lower coordination number is formed, a mechanism labeled ***D*** for **dissociation**. At the other extreme, the incoming ligand adds to the complex, and an intermediate with an increased coordination number is formed in a mechanism labeled ***A*** for **association**. Between the two extremes is **interchange, *I***, in which the incoming ligand assists in the reaction, but no detectable intermediates appear. When the degree of assistance is small and the reaction is primarily dissociative, it is called **dissociative interchange, *I_d***. When the incoming ligand begins forming a bond to the central atom before the departing ligand bond is weakened appreciably, it is called **associative interchange, *I_a***. Many reactions are described by *I_a* or *I_d* mechanisms, rather than by *A* or *D*, when the kinetic evidence points to association or dissociation, but detection of intermediates is not possible. The categories *D*, *A*, and *I* are called the **stoichiometric mechanisms**; the distinction between activation processes that are associative and dissociative is called the **intimate mechanism**. The similarities in the energy profiles for associative and dissociative reactions (**Figure 12.3**) show that unambiguously distinguishing between these mechanisms can be challenging.

Dissociation (*D*)



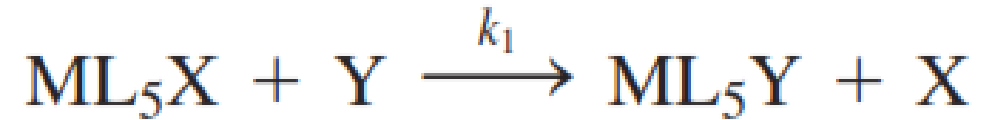
$$\frac{d[\text{ML}_5\text{Y}]}{dt} = \frac{k_2 k_1 [\text{ML}_5\text{X}][\text{Y}]}{k_{-1}[\text{X}] + k_2[\text{Y}]}$$

$$\frac{d[\text{ML}_5\text{Y}]}{dt} = \frac{k_2 k_1 [\text{ML}_5\text{X}][\text{Y}]}{k_{-1}[\text{X}]} \text{ and } \frac{d[\text{ML}_5\text{Y}]}{dt} = k_1 [\text{ML}_5\text{X}]$$

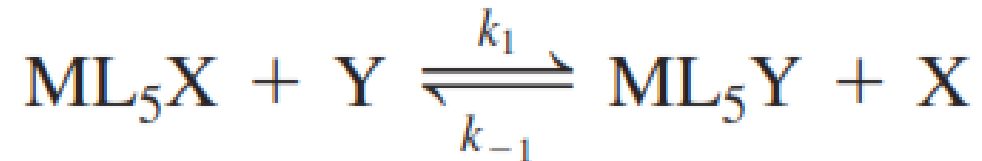
If $[\text{X}] \gg [\text{Y}]$ so that
 $k_{-1}[\text{X}] \gg k_2[\text{Y}]$

If $[\text{Y}] \gg [\text{X}]$ so that
 $k_2[\text{Y}] \gg k_{-1}[\text{X}]$

Interchange (I)



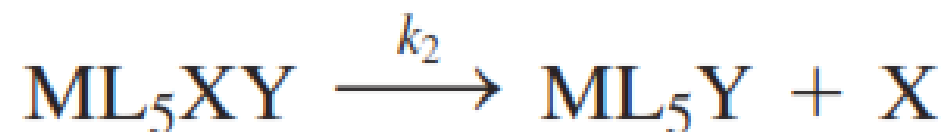
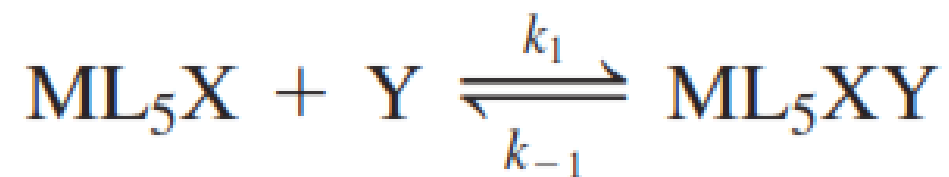
$$\frac{d[\text{ML}_5\text{Y}]}{dt} = k_1[\text{ML}_5\text{X}][\text{Y}]$$



$$-\frac{d[\text{ML}_5\text{X}]}{dt} = \frac{d[\text{ML}_5\text{Y}]}{dt} = k_1[\text{ML}_5\text{X}][\text{Y}] - k_{-1}[\text{ML}_5\text{Y}]$$

If [X] and [Y] are large

Association (A)



$$\frac{d[\text{ML}_5\text{Y}]}{dt} = \frac{k_1 k_2 [\text{ML}_5\text{X}][\text{Y}]}{k_{-1} + k_2} = k[\text{ML}_5\text{X}][\text{Y}]$$

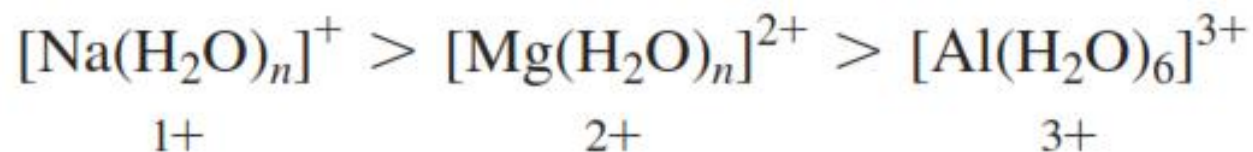
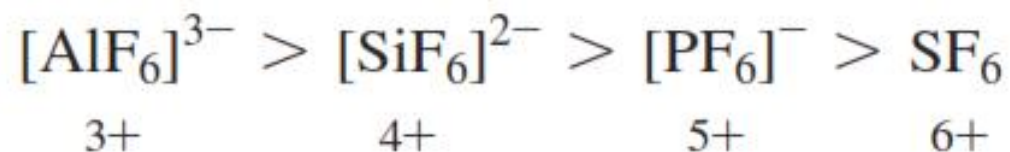
Experimental Evidence in Octahedral Substitution

Dissociation

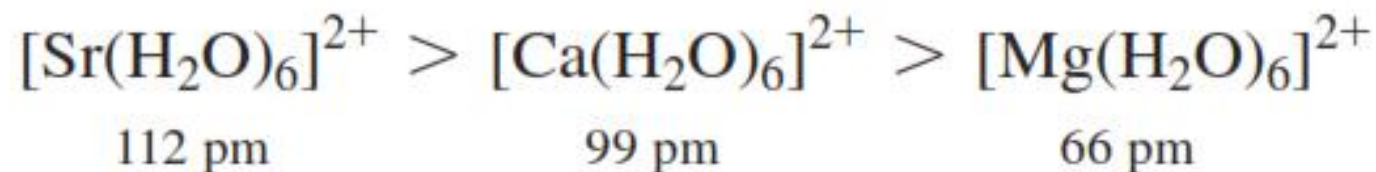
TABLE 12.3 Ligand Field Activation Energies

System	Strong Fields (units of Δ_o)			Weak Fields (units of Δ_o)		
	Octahedral LFSE	Square-Pyramidal LFSE	LFAE	Octahedral LFSE	Square-Pyramidal LFSE	LFAE
d^0	0	0	0	0	0	0
d^1	-0.400	-0.457	-0.057	-0.400	-0.457	-0.057
d^2	-0.800	-0.914	-0.114	-0.800	-0.914	-0.114
d^3	-1.200	-1.000	0.200	-1.200	-1.000	0.200
d^4	-1.600	-0.914	0.686	-0.600	-0.914	-0.314
d^5	-2.000	-1.371	0.629	0	0	0
d^6	-2.400	-1.828	0.572	-0.400	-0.457	-0.057
d^7	-1.800	-1.914	-0.114	-0.800	-0.914	-0.114
d^8	-1.200	-1.828	-0.628	-1.200	-1.000	0.200
d^9	-0.600	-0.914	-0.314	-0.600	-0.914	-0.314
d^{10}	0	0	0	0	0	0

1. *Oxidation state of the central ion.* Central atoms with higher oxidation states have slower ligand exchange rates.



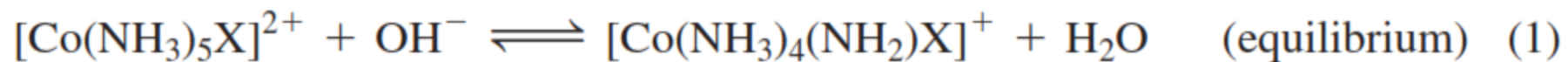
2. *Ionic radius.* Smaller ions have slower exchange rates.



1. The rate of reaction changes only slightly with changes in the incoming ligand. In many cases, **aquation** (substitution by water) and **anation** (substitution by an anion) rates are comparable. If ligand dissociation is the rate-determining step, the entering group should have no effect on the reaction rate. How much can a rate constant change before it is no longer considered comparable? Changes in rate constants of less than a factor of 10 are generally considered sufficiently similar when making these judgments.
2. Making the charge of the reactant complex more positive decreases the rate of substitution. The electrostatic attraction between the metal ion and the donor electrons of the ligands increases as the charge of the complex becomes more positive, decreasing the rate of ligand dissociation.
3. Steric crowding on the reactant complex increases the rate of ligand dissociation. When ligands on the reactant are crowded, loss of one of the ligands is made easier. On the other hand, if the reaction has an A or I_a mechanism, steric crowding interferes with the incoming ligand and slows the reaction.

4. The rate of reaction correlates with the metal–ligand bond strength of the leaving group, in a linear free-energy relationship (LFER, Section 12.4.2).
5. The volume of activation, ΔV_{act} , the change in volume on forming the activated complex, is measured by determining how much the rate constant changes as the pressure changes. Dissociative mechanisms generally result in positive values for ΔV_{act} because one species splits into two in the rate determining step, and associative mechanisms result in negative values because two species combine into one in this step, with a presumed transition state volume smaller than the total for the reactants. Caution is needed in interpreting volume effects to account for solvation effects, particularly for highly charged ions.

The Conjugate Base Mechanism



1. Base-catalyzed exchange of hydrogen from the amine groups validates the initial equilibrium (step 1).
2. The oxygen isotope ratio ($^{18}\text{O}/^{16}\text{O}$) in the product when a reaction is conducted in ^{18}O -enriched water is identical to the initial isotope ratio in the solvent ($\text{H}_2^{18}\text{O}/\text{H}_2^{16}\text{O}$), regardless of the leaving group ($\text{X}^- = \text{Cl}^-, \text{Br}^-, \text{NO}_3^-$). If an incoming water molecule had a large influence on the rate determining step (an associative mechanism), a higher proportion of ^{18}O should be in the product than in the solvent, because the equilibrium constant (K) for the reaction $\text{H}_2^{16}\text{O} + ^{18}\text{OH}^- \rightleftharpoons \text{H}_2^{18}\text{O} + ^{16}\text{OH}^-$ is 1.040.
3. RNH_2 complexes ($\text{R} = \text{alkyl}$) react faster than NH_3 complexes, possibly because steric crowding favors the 5-coordinate intermediate formed in Step 2. If the reaction had an associative mechanism, more steric bulk around the metal would be expected to lower the reaction rate.
4. The rate constants and dissociation constants for these complexes with different leaving groups form a linear free-energy relationship (LFER), in which a plot of $\ln k_{\text{OH}}$ versus $\ln K_{\text{OH}}$ is linear. This is consistent with ligand dissociation as the rate determining step.

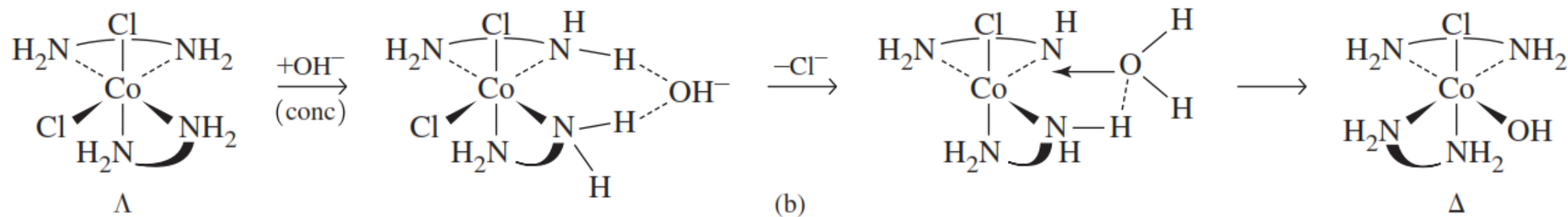
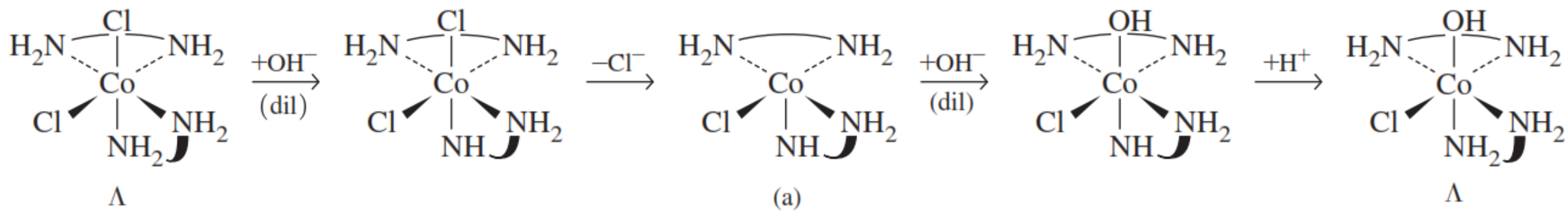
Stereochemistry of Reactions

TABLE 12.9 Stereochemistry of $[\text{Co}(\text{en})_2\text{LX}]^{n+}$ Acid Hydrolysis

$[\text{Co}(\text{en})_2\text{LX}]^{n+} + \text{H}_2\text{O} \longrightarrow [\text{Co}(\text{en})_2\text{L}(\text{H}_2\text{O})]^{(1+n)+} + \text{X}^-$					
<i>cis</i> -L	X	% <i>cis</i> Product	<i>trans</i> -L	X	% <i>cis</i> Product
OH^-	Cl^-	100	OH^-	Cl^-	75
OH^-	Br^-	100	OH^-	Br^-	73
Br^-	Cl^-	100	Br^-	Cl^-	50
Cl^-	Cl^-	100	Br^-	Br^-	30
Cl^-	Br^-	100	Cl^-	Cl^-	35
N_3^-	Cl^-	100	Cl^-	Br^-	20
NCS^-	Cl^-	100	NCS^-	Cl^-	50–70

TABLE 12.10 Stereochemistry of Base Substitution

$[\text{Co}(\text{en})_2\text{LX}]^{n+} + \text{OH}^- \longrightarrow [\text{Co}(\text{en})_2\text{LOH}]^{n+} + \text{X}^-$						
Δ - <i>cis</i> -L	X	% <i>cis</i> Product		<i>trans</i> -L	X	% <i>cis</i> Product
		Δ	Λ			
OH^-	Cl^-	61	36	OH^-	Cl^-	94
NCS^-	Cl^-	56	24	NCS^-	Cl^-	76
NH_3	Br^-	59	26	NCS^-	Br^-	81
NH_3	Cl^-	60	24	NH_3	Cl^-	76
NO_2^-	Cl^-	46	20	NO_2^-	Cl^-	6

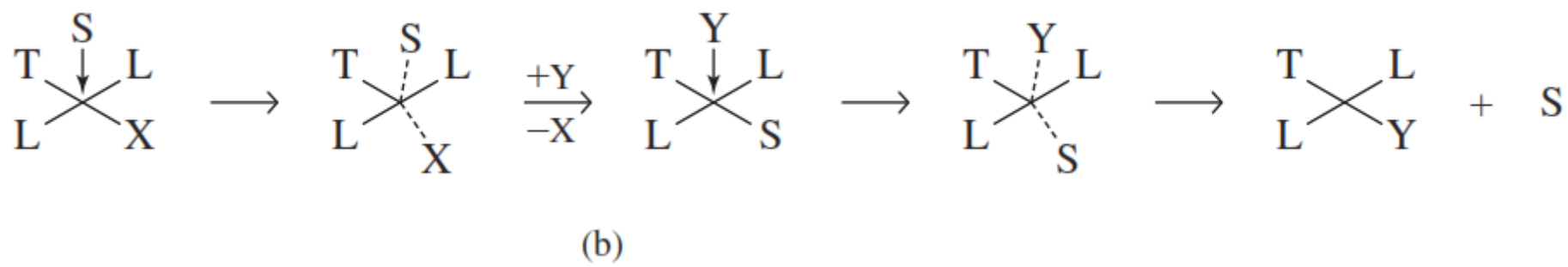
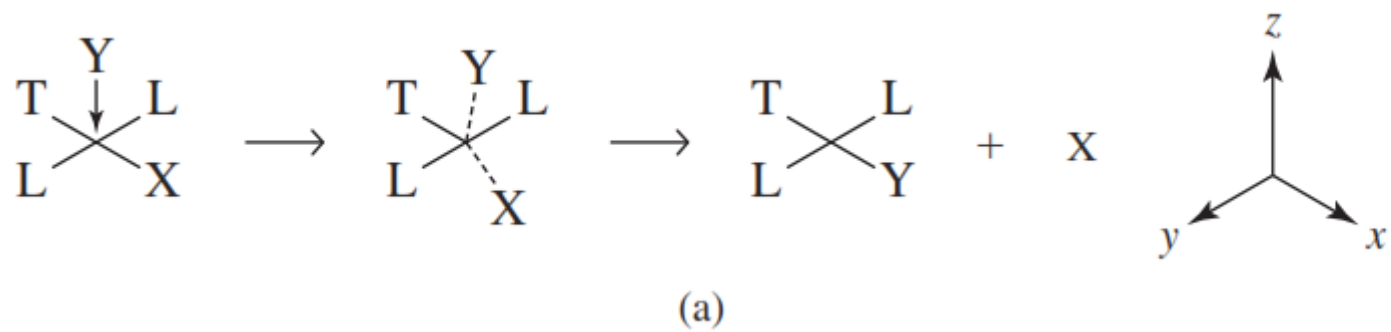


Substitution Reactions of Square-Planar Complexes



$$\text{Rate} = k_1 [\text{Cplx}] + k_2 [\text{Cplx}][\text{Y}]$$

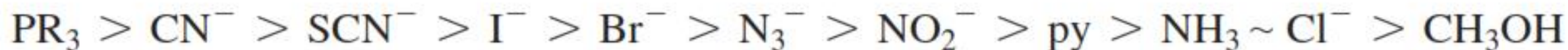
[Cplx] = concentration of the reactant complex



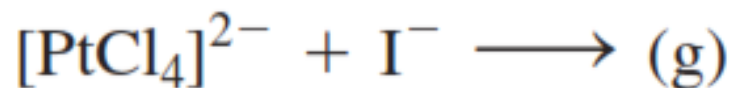
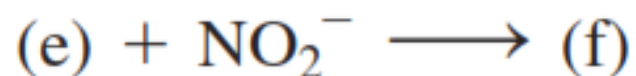
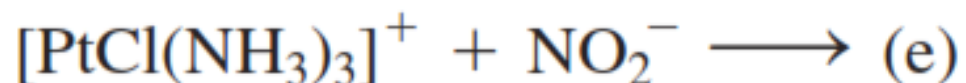
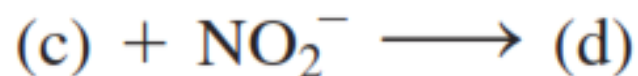
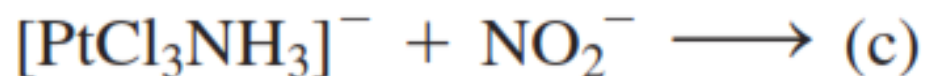
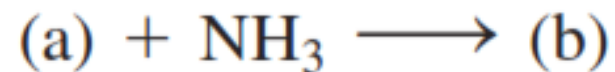
This mechanism reveals an effect of the incoming ligand. Pt(II) is a soft acid, so soft ligands react more readily with it. The order of ligand reactivity depends somewhat on the other ligands on the Pt, but the rate constants for



for different Y in methanol rank as follows (**Table 12.12**):



The *trans* Effect



order for the *trans* influence on the basis of the relative σ -donor properties of the ligands:



The order of ligand π -acceptor ability is



The overall *trans* effect list is the result of the combination of the two effects:

